Lookback times, horizons and photon paths for various Friedmann–Lemaître–Robertson–Walker cosmological models

By

SURYA SHANKAR R

(Reg.No.: I18PH039)

A dissertation submitted in partial fulfillment of the requirements to the Department of Physics,

for the degree of

Master Of Science

(Five Year Integrated Program)

in

Physics

Under the supervision of

Dr. Lukáš Richterek,

Palacký University Olomouc, Czech Republic.

and

Dr. Ajay Kumar Rai,

Sardar Vallabhbhai National Institute of Technology, Surat, India.

Department of Physics,

Sardar Vallabhbhai National Institute of Technology,

(An Institute of National Importance, NIT Act 2007)

Surat-395007, Gujarat, INDIA.

APPROVAL

Dissertation entitled "**Lookback times, horizons and photon paths for various Friedmann–Lemaître–Robertson–Walker cosmological models**" by **Surya Shankar R** is approved for the degree of Master of Science in Physics.

Dr. Vikas Kumar Ojha
(Examiner 1)

Dr. Dipika Patel
(Examiner 2)

Dr. Dimple V. Shah
(Head Of Department)

Dr. Ajay Kumar Rai
(Supervisor)

Date: 6th June, 2023

Place: Surat, Gujarat, India

Department of Physics,

Sardar Vallabhbhai National Institute of Technology,

(An Institute of National Importance, NIT Act 2007)

Surat-395007, Gujarat, INDIA.

DECLARATION

I hereby declare that the dissertation entitled "**Lookback times, horizons and photon paths for various Friedmann–Lemaître–Robertson–Walker cosmological models**" is a genuine record of research work carried out by me and no part of this dissertation has been submitted to any University or Institution for the award of any degree or diploma.

Surya Shankar R

(Reg. No. I18PH039)

Department of Physics,

Sardar Vallabhbhai National Institute of Technology,

Surat- 395007.

Date: 6th June, 2023

Place: Surat, Gujarat, India

Department of Physics,

Sardar Vallabhbhai National Institute of Technology,

(An Institute of National Importance, NIT Act 2007)

Surat-395007, Gujarat, INDIA.

CERTIFICATE

This is to certify that the dissertation entitled "**Lookback times, horizons and photon paths for various Friedmann–Lemaître–Robertson–Walker cosmological models**" is a bona fide record of research work done by **Mr. Surya Shankar R** from **Sardar Vallabhbhai National Institute of Technology, Surat**. He carried out the study reported in this dissertation, independently under my co-supervision. I also certify that the subject matter of the dissertation has not formed the basis for the award of any Degree or Diploma of any University or Institution.

Dr. Ajay Kumar Rai

Associate Professor,

Department of Physics,

Sardar Vallabhbhai National Institute of Technology,

Surat- 395007.

Date: 6th June, 2023

Place: Surat, Gujarat, India

Faculty of Science

Department of Experimental Physics, Faculty of Science, Palacký University Olomouc
✉ 17. listopadu 1192/12, CZ–771 46 Olomouc, Czech Republic, Europe
☎ *phone:* (+420) 585 634 104
✉ *e-mail:* lukas.richterek@upol.cz
www: http://muj.optol.cz/~richterek

Letter from External Guide

To whom it may concern

This is to certify that the work in this dissertation titled *Lookback times, horizons and photon paths for various Friedmann–Lemaı̆tre–Robertson–Walker cosmological models* concerning numerical calculations of some characteristic of selected cosmological models has been successfully carried out by *Mr. Surya Shankar Rajendra Kumar* (Reg.No. I18PH039) at Palacký University Olomouc, Czech Republic, under my supervision from February 20, 2023 to May 8, 2023. I certify that the record of this dissertation work is original. The student has been working with great interest in the topics, enthusiasm and stand-alone. For any further inquiries, please do not hesitate to contact me.

Olomouc, May 31, 2023

UNIVERZITA PALACKÉHO V OLOMOUCI
PŘÍRODOVĚDECKÁ FAKULTA
KATEDRA EXPERIMENTÁLNÍ FYZIKY
tř. 17. listopadu 12, 771 46 Olomouc
-1-

Faithfully,

Mgr. Lukáš Richterek, Ph.D.
assistant lecturer

ഹരി ശ്രീ ഗണപതയേ നമ:

Acknowledgements

I want to start by expressing my sincere gratitude to my dissertation supervisor (research), Dr. Lukáš Richterek, for his unwavering support throughout my Integrated Masters's program and related research, for enlightening me with his thoughts and experience, for granting me a great deal of freedom during the research work, and for the countless discussions during the course. He is an important influence on how I currently perceive and approach my research, and I couldn't have asked for a greater mentor, colleague, and supervisor for my study and for life in general.

At the Sardar Vallabhbhai National Institute of Technology in Surat, I would like to express my gratitude to Dr. Ajay Kumar Rai for serving as my official dissertation supervisor. I would also like to thank the entire faculty at S.V.N.I.T., Surat, Department of Physics for their assistance during my program. I owe a debt of gratitude to Prof. Farhad Ali, Prof. Rashmi Uniyal, Dr. Dimple Shah, and others for serving as my coworkers and project supervisors throughout the brief internships. I also like to express my gratitude to Palacky University in Olomouc's Department of Experimental Physics for their gracious hospitality throughout my visit.

I want to thank my friends Niharika Ahirekar and Vyshakh Varrier for investing their valuable time with me over various important discussions about this work. I also want to thank Dashamoolam Hamdan, Ajay Francis, Geethika Rajan, Anusree CB, Gaadha Lekshmi, Rashi Kaimal and Foram Fanasia for making my time at our institute memorable. The constant encouragement and support of my parents and sister, without whose efforts none of this would have been possible, I would not have taken up research or persevered through the difficulties. Last but not least, I want to thank Niharika Ahirekar for supporting me and standing by me with constant encouragement through adversities.

Contents

List of Figures

Chapter 1

Introduction

Einstein's General Theory of Relativity has an exact solution known as the Friedmann-Lemaître-Robertson-Walker (FLRW) metric. General relativity, which Albert Einstein first proposed in 1915, is the geometric theory of gravitation that is currently used to explain gravitation in modern physics. (see e.g. [1]).The theory of general relativity, which generalises the theory of special relativity and enhances Newton's law of universal gravitation, offers a cogent explanation of gravity as a geometric property of space and time, or four-dimensional spacetime. In particular, the curvature of spacetime directly affects the energy and momentum of all the matter and radiation that is present. The relationship is defined by the set of second-order partial differential equations known as the Einstein field equations.

The metrics of standard cosmological models describe exact solutions of Einstein's equations; in the simplest cases with the metric describing an expanding universe, which is homogeneous and isotropic (mathematically speaking, they can be used to describe a contracting universe as well). Our real Universe seems to be described best by the ΛCDM model, which is commonly known as the Standard Model of Modern Cosmology. From experimental results (see e.g. [2, 3]), we know that the expansion of the universe is accelerating, and the further we observe, the faster the universe is expanding, to the point that we have a boundary for the *"observable universe"* because the universe has inflated faster than the speed of light, creating a horizon, known as the Hubble sphere.

The difference between the age of the universe at the time of observation, t_0, and the age of the universe at the time of photon emission, t_e, is the lookback time, t_{lb}, to an object. With evolutionary models, it is used to forecast characteristics of high-redshift objects, such as passive stellar evolution for galaxies.

A gravitational horizon in general relativity is a hypothetical 3-d spherical surface beyond which all null geodesics keep receding away from the observer on the account of expansion of space. (also known as the *"apparent horizon"*). The idea of the horizon is usually introduced in connection with the black hole spacetimes. The radius of the apparent horizon R_h is computed according to the metric and calculated in terms of the metric and model of general relativity used. The apparent horizon of the Universe is not static, in contrast to that of the Schwarzschild and Kerr metrics, which are metrics of a stationary black hole and rotating black holes, respectively. The cosmic fluid may eventually change into an event horizon, an asymptotically defined surface that permanently separates events that are causally connected from those that are not, depending on the equation of state of the fluid.

The paths of photons in FLRW cosmology are determined by the null geodesics, which are the curves in spacetime along which the interval $ds^2 = 0$. Since photons travel at the speed of light, their paths follow null geodesics. To analyze the photon path ψ, we consider a specific case where the photon is emitted from a source and propagates through an expanding universe. As the photon travels, the spacetime it traverses also expands. The scale factor determines the expansion rate of the universe, which can vary with time. Photon paths are hence closely associated with the very nature of the model of the universe as well as the proper distances between sources and observers. The objectives of this work include finding horizons, redshifts, distances, and lookback periods for cosmic objects in various FLRW cosmology models as well as calculating and displaying the photon routes in those models graphically, notably for chosen illustrative models for various scenarios. The corresponding differential equations and integrals were computed numerically by relatively simple Euler's method implemented in PyLab procedural interface using Python as a high-level, general-purpose programming language.

Chapter 2

General Relativity and Cosmological Models

General Relativity is a crucial building block of modern physics. It utilizes the ability of space and time to *"curve"* as an explanation for gravity. In other words, it links gravity to the changing geometry of spacetime to explain gravity in terms of how space and time may *"bend"*. It is also known as Einstein's theory of gravity and the general theory of relativity. In 1915, Albert Einstein developed his *"general"* theory of relativity after first developing a "special" theory in which he made the assumption that the laws of physics apply regardless of the inertial frame of reference.When Einstein tried to incorporate accelerating masses into his special theory, he came to the conclusion that there must be some interaction between mass and the spacetime that causes the mass to appear to exert a force on other masses. It seems that matter drags the fabric of spacetime that it occupies, producing a *"curve"* that forces other nearby matter to slide toward it.

The Einstein field equation [4]:

$$G_{\mu\nu} + \Lambda g_{\mu\nu} = \kappa T_{\mu\nu}, \tag{1}$$

where $G_{\mu\nu}$ is defined as Einstein tensor, $g_{\mu\nu}$ is defined as metric tensor, and $T_{\mu v}$ is defined as stress-energy tensor. Λ is the cosmological constant and κ is the Einstein gravitational

constant. The Einstein tensor is expressed as:

$$G_{\mu\nu} = R_{\mu\nu} - \frac{1}{2}Rg_{\mu\nu}, \tag{2}$$

where $R_{\mu\nu}$ is the Ricci curvature tensor, and R is the scalar curvature. Mathematically, the Einstein gravitational constant is defined as $\kappa = \frac{8\pi G}{c^4} \approx 2.07664 \times 10^{-43}\ \mathrm{N}^{-1}$, where G is the Newtonian constant of gravitation and c is the speed of light in vacuum. Therefore the Einstein Field Equation can also be expressed as

$$R_{\mu\nu} - \frac{1}{2}Rg_{\mu\nu} + \Lambda g_{\mu\nu} = \kappa T_{\mu\nu}. \tag{3}$$

The Friedmann–Lemaître–Robertson–Walker (FLRW) metric [5], which is an exact solution of Einstein's field equation, describes a universe that is *"expanding"*. As a result, the size of space itself expands intrinsically. It is not necessary for space to exist *"outside"* of the universe or for it to extend *"into"* anything. The metric (which controls the size and geometry of spacetime itself) changes in scale rather than space or the things in space *"moving"* in the conventional sense. As the spatial component of the universe's spacetime metric scales up, objects move farther away from one another at ever-increasing speeds. Any observer in the universe would see that space is expanding everywhere and that galaxies are moving away from it at rates proportional to their distance from the observer, with the exception of the nearest galaxies, which are gravitationally bound. The fact that objects in space cannot move faster than light does not restrict the implications of changes in the metric itself. The size of the observable universe is constrained as the universe expands, so objects that move past the cosmic event horizon eventually stop being observable. The universe's expansion is the increase in distance over time between any two specific gravitationally unbound regions of the observable universe.

An absolute horizon [6] is a boundary in spacetime that is defined with respect to the outside universe and outside of which events cannot be perceived by an outside observer, while the farthest distance from which light from particles may have reached the observer during the early universe's history is known as the particle horizon, also known as the

cosmic horizon. Its distance at the current epoch determines the size of the observable universe because it serves as the boundary between the cosmos' observable and unobservable portions.

In FLRW cosmology, it is possible to calculate lookback time, the age of the universe, and luminosity distance vs redshift analytically by expressing them in terms of a limited set of elementary functions. Using examples and the integration theorem of Chebyshev, we categorize these circumstances. Lookback time [8] for the most distant objects can be used to estimate the age of the universe. As realistic models predict that the universe is expanding and accelerating, and the lookback time can be used to measure this expansion.

Horizons represent a boundary beyond which information cannot travel due to the finite speed of light. Horizons are an important concept in cosmology. The cosmic horizon is defined as the maximum distance that light can travel since the Big Bang. This can be used to determine the maximum observable distance and thus the extent of the observable universe. The path of photons is the trajectory of light from the Big Bang to the present day and is the basis for how light from distant galaxies is observed on Earth. Photon paths trace the history of the universe and provide insight into the FLRW model of the universe.

Photon paths [7] provide a visual representation of the way light moves through the universe and the lookback time is the length of the time it takes for light to reach us from a distant source. By taking the properties of such models into account, we can gain valuable insights into the structure, evolution, and fate of our universe.

Thus, the FLRW cosmological models provide an excellent framework for understanding the evolution of the universe. These models describe the universe as a dynamic, expanding spacetime with a homogeneous matter-energy content. This can be used to explore the impact of different cosmological parameters, such as the Hubble constant, on the cosmic horizon, the path of photons, and the lookback time. By studying these models characteristics, we can gain valuable insight into the history of the universe.

The aim of the work is to calculate and graphically present the photon paths in various FLRW cosmological models, find horizons, redshifts, distances, and lookback times for cosmological objects in those models, especially for selected illustrative models for different scenarios (namely, today's benchmark model or the Λ Cold Dark Matter (ΛCDM) model, the Einstein-de Sitter model, Big Crunch model, loitering universe model, empty universe, Big Bounce model and Pure Lambda model).

The Lambda Cold Dark Matter (ΛCDM) model [9] is a widely accepted cosmological theory that explains the universe's creation and development. According to this theory, there are three main elements that make up the universe: dark matter, baryonic matter, and dark energy. The term "Λ" in the name refers to the cosmological constant, which Einstein coined in his theory of general relativity to explain the universe's apparent acceleration. The cosmological constant is equivalent to a type of dark energy that is evenly dispersed throughout the universe and acts as an attractive force on matter, speeding up the universe's expansion. The cold dark matter component of the ΛCDM model, a type of non-baryonic matter thought to account for the majority of the universe's matter, is included in contrast to the baryonic matter component, which includes all the familiar forms of matter like stars, planets, and gas clouds. According to a number of observations, the universe (and this most realistic cosmological model) is made up of roughly 5% ordinary matter, 27% dark matter, and 68% dark energy (different sources may give slightly different values). [2, 3]). According to the model, the early universe experienced inflationary expansion, radiation dominance, and then matter dominance. According to the model, galaxy formation occurs hierarchically, and that over time, massive galaxies like the Milky Way must have absorbed 100 or more dwarf galaxies through minor mergers. The cosmological constant, a type of dark energy, is associated with a negative pressure that becomes more significant over time as the universe expands. Our understanding of the universe has significantly improved thanks to the model, which is supported by a variety of observational data. (see e.g. [4]).

The Einstein-de Sitter universe [10] is a cosmological model proposed by Albert Einstein and Willem de Sitter in 1932. It assumes a flat, matter-only universe with no spatial

curvature or cosmological constant. This model became a standard for many years due to its simplicity, but observations of the accelerating universe and the Hubble constant in the 1990s led to problems with this model. The modern ΛCDM model includes dark energy and cold dark matter, and the Einstein-de Sitter model is now considered a good approximation of our universe according to the model, the early universe experienced inflationary expansion, radiation dominance, and then matter dominance. The cosmological constant, a type of dark energy, is associated with a negative pressure that becomes more significant over time as the universe expands. Our understanding of the universe has significantly improved thanks to the model, which is supported by a variety of observational data such as in the past, well after the radiation-dominated era but before dark energy became important. The Einstein-de Sitter model describes the expansion of the matter-dominated universe and it defines the critical density with which we compare the amount of matter in the universe. Because of its simplicity (it can be solved analytically) it has also a great pedagogical value and usually serves as a first model to introduce the dependency of the measured and model-based characteristics.

The Big Crunch cosmological [11] model is a theoretical scenario for the ultimate fate of the universe. It is based on the idea that the universe will stop expanding and begin to contract due to the gravitational attraction of matter. As the universe contracts, it will become denser and denser and hotter until it eventually collapses into a singularity, similar to the Big Bang. The Big Crunch model can assume that the universe is open, closed, or flat and has a finite amount of matter in a finite volume. However, recent observations suggest that the universe is flat (or, more carefully said, very close to this geometry) and that its expansion is accelerating, which makes the Big Crunch unlikely. Instead, the most accepted theory today is the heat death of the universe, where the universe will continue to expand and become increasingly cold and dark.

The idea of the Loitering Universe model [12] is a theoretical model and was proposed in various contexts in 1993 by physicists Lawrence M. Krauss and Glenn D. Starkman. Their model suggests that the universe is flat, but with a very low density of matter, causing it to expand at an ever-slowing rate. Within this work, the term “loitering”

refers to the fact that the universe's parameters may be theoretically tuned in this way so that the expansion rate is so small within a long time that it appears to be almost standing still. In other words, it is a type of closed universe model in cosmology where the universe remains close to the static Einstein universe for a significant period of time before re-expanding. This model is characterized by a significant cosmological constant and is one of several closed universe models, each with different features and characteristics that affect the age of the universe and density perturbations.

Similarly, the concept of the Big Bounce model has been introduced in various contexts (see e.g. [13]). Some of them come with a cosmological model that suggests the universe undergoes cycles of expansion and contraction. Such a Big Bounce model has become a topic of active investigation again due to potential problems with inflation theory, and it has found support in loop quantum gravity. In this model, the universe's behavior and fundamental physical constants may change during contraction and expansion. While the Big Bounce theory was initially proposed as a phase of the cyclic model, it has gained popularity as a standalone model to explain the origins of the universe. One prediction of the Big Bounce Universe model is that it should lead to a more homogeneous and isotropic universe, with fewer large-scale structures than in the previous cycle. Observations of the cosmic microwave background radiation can help determine whether the Big Bounce Universe model is a viable explanation for the universe's origins. Within this work, we take the Big Bounce model as a theoretical example of a closed universe that did not start with the Big Bang; on the contrary, it is shrinking from large scales and – at one moment – it starts to expand. Compared with the Loitering universe, it is caused by a higher value of the positive cosmological constant Λ ("dark energy").

The term "Pure Lambda Universe" refers to a specific type of cosmological model also known as the de Sitter Universe model. In fact, it is a specific case of the ΛCDM model, but for the Pure Λ universe or the de Sitter Universe, we assume the universe is composed of only "dark energy" or just a non-zero cosmological constant, which results in accelerated expansion. It is sometimes also used as and approximation for the inflation epoch in the very early universe [14]. The ΛCDM model has received strong support from

observations of the cosmic microwave background radiation [15], large-scale structure, and supernovae. It is crucial to keep in mind that the model is not ideal and that some problems, including the nature of dark matter and the precise value of the cosmological constant, remain unanswered.

The Planck [3] and Pantheon missions are involved in research on the creation and growth of the universe. The Cosmic Microwave Background (CMB), or ancient radiation from the Big Bang, was the focus of the European Space Agency's Planck space telescope mission. The mission's goal was to learn more about the universe's beginning and long-term evolution. A project called the Pantheon survey [16] aims to measure the characteristics of dark energy, which is thought to be the cause of the universe's accelerating expansion. It makes use of information from several cosmological surveys, including the Supernova Cosmology Project and the Dark Energy Survey. The ΛCDM model is supported by the Planck+Pantheon result, which is completely compatible with the luminosity.

The lookback times graphs we are going to construct in the following chapters, illustrate the relationship between lookback time and matter content, revealing distinct patterns for models like the Loitering universe and the Rebouncing model, while most others exhibit a similar structure. Notably, even the empty universe and Pure Lambda universe show generic graphs. In the Rebouncing model, the graph shows an increase followed by a decrease in redshift, indicating a future collapse with a negative scale factor. In the generic models, low redshifts correspond to recent times, while higher redshifts signify older observed objects. The graph slope may initially steepen, and at larger redshifts, the lookback time significantly increases, representing light from early cosmic epochs. A graphical representation of the evolution of apparent horizons in time depicts linear increasing radii for the Einstein-de Sitter model, constant radii for the Pure Lambda universe and an increasing then plateau-shaped graph for the ΛCDM model. The photon paths show the expansion of the universe and how it stretches through the course of its journey through spacetime. The following chapters contain brief mathematical descriptions of the details mentioned above.

Chapter 3

FLRW Metric and Lookback times

3.1 Mathematical expressions for FLRW Metric

The Friedmann Robertson-Walker (FLRW) metric is given by . (e.g. [4]):

$$ds^2 = c^2dt^2 - a^2(t)\left[\frac{dr^2}{1-kr^2} + r^2\left(d\theta^2 + \sin^2\theta d\phi^2\right)\right]. \tag{4}$$

For the coordinate system used in this metric, for the comoving radius, r, and cosmic time t, $a(t)$ is the expansion factor measured by a comoving observer (and constant everywhere). In a closed spherical world, k is 1, in a flat universe, it is 0, and in an open universe, it is -1. Alternatively, the metric element in Eq. (4) can be transformed into a more convenient form for the radial motion description

$$ds^2 = c^2dt^2 - a^2(t)\left[d\psi^2 + S_k(\psi)^2\left(d\theta^2 + \sin^2\theta d\phi^2\right)\right], \tag{5}$$

where the function $S_k(\psi)$ depends on constant spacetime curvature k and the radius of curvature R_0

$$S_k(\psi) = \begin{cases} R_0 \sin\left(\dfrac{\psi}{R_0}\right) & \text{for } k = 1 \\ \psi \equiv r & \text{for } k = 0 \\ R_0 \sinh\left(\dfrac{\psi}{R_0}\right) & \text{for } k = -1 \end{cases} \tag{6}$$

We shall see that the coordinates indicate the viewpoint of "a free-falling observer," similar to—and perfectly consistent with—the free-falling observer in the Schwarzschild and Kerr spacetimes. This is one of the many facets of the FLRW metric that we shall investigate throughout this work. We will find it very insightful to express the FLRW metric in terms of coordinates that can be used to describe a fixed position relative to the observer in the cosmological context, just as it makes sense and is advantageous to cast the latter in a form relevant to the accelerated observer as well, such as one at rest with respect to the source of gravity.

The proper radius R can be defined as:

$$R(t) \equiv a(t)r. \tag{7}$$

Proper radius is frequently used to represent the changing distance that increases as the universe expands rather than the comoving distance r between two places. This definition of R actually follows directly from Weyl's postulate [17], which states that, no two worldlines can ever cross after the big bang for the cosmological principle to hold from one time-slice to the next, with the exception of any local unusual motion that may occur on top of the averaged Hubble flow. This condition specifies that any distance in an FLRW cosmology must be expressible as the result of an independent universal function of time, $a(t)$ and a constant comoving length r. In some situations, R is referred to as the areal radius - the radius of two-spheres of symmetry - defined in a coordinate-independent way by the relation $R \equiv \sqrt{A/4\pi}$, where A is the area of the two-sphere in the symmetry. These two definitions of R are, of course, fully self-consistent with each other.

For the FLRW metric given by eq. (4), we have the well-known results known as the Friedmann equations of motion,

$$\begin{aligned}
H^2 &= \left(\frac{\dot{a}}{a}\right)^2 = \frac{8\pi G}{3}\rho - \frac{kc^2}{a^2} = \frac{8\pi G}{3c^2}\varepsilon - \frac{kc^2}{a^2}, \\
\frac{\ddot{a}}{a} &= --\frac{4\pi G}{3}\left(\rho + \frac{3P}{c^2}\right) = -\frac{4\pi G}{3c^2}\left(\varepsilon + 3P\right) \\
\dot{\rho} + 3H\left(\rho + \frac{P}{c^2}\right) &= 0 \quad \text{or} \qquad \dot{\varepsilon} + 3H(\varepsilon + P) = 0
\end{aligned} \tag{8}$$

where $H = \frac{\dot{a}}{a}$ is the Hubble Parameter, where an overdot, as usual, denotes a derivative with respect to t. Here, ρ and P represent, respectively, the total matter density and total pressure in the comoving frame, assuming the perfect fluid form of the stress-energy tensor, Alternatively, $\varepsilon = \rho c^2$ is the energy density. An important role plays the equation of state for the considered material. Usually it is presented in the form $P = w\varepsilon = w\rho c^2$, where w is the constant.

3.2 Lookback times

We are able to exactly determine the lookback time, appropriate distance of observed objects, and age of the universe for a specific model using FLRW cosmology. Integrals that take the form of infinite hypergeometric series are used to express these quantities, which are of utmost importance for contemporary cosmology. In a certain cosmological model, lookback time, age, and proper distance can all be computed numerically. Even so, it would be helpful to know when these quantities can also be estimated analytically in terms of a constrained number of simple functions. This simplification results from the truncation of the hypergeometric series expressing them. When the integral representing lookback time, age, or luminosity distance has a specific shape that is taken into consideration by the Chebyshev theorem of integration [18], it occurs equivalently.

We start with Friedmann's equations Eq. (8) of motion with a non-zero cosmological constant Λ.

$$\begin{aligned} H^2 &= \frac{8\pi G}{3}\rho + \frac{\Lambda c^2}{3} - \frac{kc^2}{a^2}, \\ \frac{\ddot{a}}{a} &= -\frac{4\pi G}{3}\left(\rho + \frac{3P}{c^2}\right) + \frac{\Lambda c^2}{3}, \\ \dot{\rho} &+ 3H\left(\rho + \frac{P}{c^2}\right) = 0. \end{aligned} \tag{9}$$

where vacuum energy density and vacuum pressure contributed by the non-zero cosmological constant can be expressed as

$$\varepsilon_\Lambda = \rho_\Lambda = \rho_\Lambda c^2 = -\frac{c^2}{8\pi G}\Lambda = -P_\Lambda$$

The third Friedmann equation can also be expressed as

$$\frac{\dot{\rho}}{\rho} + 3\frac{\dot{a}}{a}(1+w) = 0, \tag{10}$$

Which is equivalent to,

$$\frac{d}{dt}[\ln \rho + 3(1+w)\ln a] = 0. \tag{11}$$

Meaning the conservation equation is given as,

$$\rho(a) = \rho_0 \left(\frac{a_0}{a}\right)^{3(1+w)} \tag{12}$$

where ρ_0 is a constant. Suppose that the cosmic fluid is a mixture of n non-interacting fluids with individual energy densities ρ_i and pressures P_i, with $P_i = w_i \rho_i c^2$ and $w_i =$ const. $(i = 1, 2, 3, \ldots, n)$. The total energy density and pressure are

$$\rho_{(\text{tot})} = \sum_{i=1}^{n} \rho_i, \quad P_{(\text{tot})} = \sum_{i=1}^{n} w_i \rho_i c^2, \tag{13}$$

respectively.

From the first Friedmann equation given by eq. (9), we can see that,

$$\frac{kc^2}{a^2 H^2} = \frac{8\pi G}{3H^2}\rho + \frac{\Lambda c^2}{3H^2} - 1. \tag{14}$$

By setting the normalized spatial curvature, k, to zero and assuming that Λ is equal to zero (as it is for all fundamental Friedmann universes), it is possible to find a formula for the critical density. We obtain the first of the Friedmann equations when the substitutions are used. 1

$$\rho_{\text{c}} = \frac{3H^2}{8\pi G} = c^2 \tag{15}$$

and introducing the dimensionless value

$$h = \frac{H_0}{100 \ \text{km/s/Mpc}}, \tag{16}$$

we find for $H_0 = 67.4$ km/s/Mpc, i.e. $h = 0.674$:

$$\rho_{\rm c} = \frac{3H^2}{8\pi G} \approx 1.8788 \times 10^{-26} h^2 \text{ kg m}^{-3} \approx 7.8 \times 10^{-10} h^2 \text{ J m}^{-3}, \tag{17}$$

The density parameter is thus given as follows, which is useful for comparing various cosmological models:

$$\Omega_\rho \equiv \frac{\rho}{\rho_c} = \frac{8\pi G}{3H^2}\rho \tag{18}$$

This expression was initially employed to calculate the universe's spatial geometry, where ρ_c stands for the critical density at which the universe's spatial geometry is flat (or Euclidean). If Ω is greater than unity, the universe's space sections are closed; assuming a zero vacuum energy density, the cosmos will eventually stop expanding and collapse. They are open and the universe continues to grow indefinitely if Ω is less than unity. The spatial curvature and vacuum energy terms, however, can alternatively be combined into a more general expression for Ω, in which case this density parameter equals exactly one. The following step involves measuring the various components, which are typically identified by subscripts.

According to the Λ-CDM model, baryons, cold dark matter, and dark energy are significant parts of Ω. The WMAP spacecraft has determined that the universe's spatial shape is almost flat. It follows that a model with a spatial curvature parameter k of zero can accurately represent the universe. This may merely hint that Universe is much greater than what we can observe; it does not necessarily mean that the universe is infinite.

Therefore, eq. (14) can be written as

$$\frac{kc^2}{a^2} = H^2 \left(\Omega_\rho + \Omega_\Lambda - 1\right), \tag{19}$$

where we define

$$\Omega_\Lambda = \frac{\Lambda c^2}{3H^2} \quad \text{and} \quad \Omega_k = \frac{kc^2}{H^2}.$$

If we consider present-day values, for $t = t_0$, eq. (14) can be written as

$$\begin{aligned} \frac{kc^2}{a_0^2 H_0^2} &= \frac{8\pi G}{3H_0^2}\rho_0 + \frac{\Lambda c^2}{3H_0^2} - 1 \\ or & \\ \frac{kc^2}{a_0^2} &= H_0^2\left(\Omega_{\rho 0} + \Omega_{\Lambda 0} - 1\right) \end{aligned} \tag{20}$$

Substituting $\rho(a)$ from eq. (12) into the first Friedmann equation eq. (9), we get

$$\dot{a}^2 = a^2\left[\frac{8\pi G}{3}\rho_0\left(\frac{a_0}{a}\right)^{3(1+w)} + \frac{\Lambda c^2}{3} - \frac{kc^2}{a^2}\right] \tag{21}$$

$$\implies \dot{a}^2 = \frac{8\pi G}{3}a_0^2\rho_0\left(\frac{a_0}{a}\right)^{(1+3w)}\left(\frac{a^2}{a_0^2}\right) + \frac{\Lambda c^2 a_0^2}{3}\left(\frac{a^2}{a_0^2}\right) - a_0^2 H_0^2\left(\Omega_{\rho 0} + \Omega_{\Lambda 0} - 1\right)$$

Here, $\Omega_{\rho 0} + \Omega_{\Lambda 0} = \Omega_0^{(\mathrm{tot})}$

$$\begin{aligned} \therefore \dot{a} &= \sqrt{\frac{8\pi G}{3}a_0^2\rho_0\left(\frac{a_0}{a}\right)^{3w+1} - \left(\Omega_0^{(\mathrm{tot})} - 1\right)a_0^2 H_0^2 + \frac{\Lambda c^2 a_0^2}{3}\left(\frac{a_0}{a}\right)^{-2}} \\ &= a_0 H_0\sqrt{\frac{8\pi G}{3H_0^2}\rho_0\left(\frac{a_0}{a}\right)^{3w+1} - \left(\Omega_0^{(\mathrm{tot})} - 1\right) + \frac{\Lambda c^2}{3H_0^2}\left(\frac{a_0}{a}\right)^{-2}} \\ &= a_0 H_0\sqrt{1 - \Omega_0^{(\mathrm{tot})} + \Omega_{\rho 0}(z+1)^{3w+1} + \Omega_{\Lambda 0}(z+1)^{-2}}, \end{aligned} \tag{22}$$

where the relationship between the scale factor $a(t)$ and redshift z is given by:

$$z = \frac{a_0}{a} - 1. \tag{23}$$

This implies also

$$da = -\frac{a_0}{(z+1)^2}dz$$

In cosmology, redshift is a phenomenon that occurs due to the expansion of the universe. It refers to the shift of light towards longer wavelengths, which corresponds to a decrease in frequency, as the universe expands. Redshift is an essential tool for understanding the dynamics and evolution of the universe. The redshift of an astronomical object is denoted by z and is defined as the change in the wavelength (λ) of light emitted by the object, relative to its observed wavelength (λ_0). Mathematically, the relationship between

redshift and wavelength is given by:

$$1 + z = \frac{\lambda}{\lambda_0} \tag{24}$$

This equation, which expresses the relative change in wavelength, shows that redshift is a dimensionless quantity. The perceived wavelength is longer than the emitted wavelength when z is positive, which denotes a redshift. In contrast, a negative z value indicates a blueshift, which means the seen wavelength is less than the wavelength being emitted. However, redshift is primarily utilised in cosmology as a gauge of the universe's expansion, leading to longer observable wavelengths. We must take into account the cosmological principle and the idea of the scale factor in order to comprehend the connection between redshift and the universe's expansion.

Eq. (23) indicates that as the universe expands ($a(t)$ increases), the redshift of light emitted from distant objects also increases. Conversely, if the scale factor were to decrease, indicating a contraction of the universe, the redshift would decrease, leading to a blueshift. However, observations have consistently shown that the universe is expanding, resulting in redshifted light from distant sources. Overall, redshift in cosmology is a consequence of the expansion of the universe, causing the observed light from distant objects to be stretched to longer wavelengths. It is a fundamental observational tool used to study the dynamics, structure, and evolution of the cosmos.

Coming back to our discussion on deriving lookback times, we consider universes beginning with a Big Bang $a(0) = 0$ at $t = 0$ and we denote the present value of time-dependent quantities with a zero subscript. Then, since $\dot{a} = da/dt$, the lookback time to a source that emitted at time t_e, scale factor a_e, and redshift z_e is

$$t_{lb} = \int_{t_e}^{t} dt' = \int_{a_e}^{a_0} \frac{da'}{\dot{a}'} \tag{25}$$

In the limit $t_e \to 0$ (or $a_e \to 0$, or $z_e \to +\infty$), one obtains the age of the universe

$$\begin{aligned} t_0 &= \int_0^t dt' \\ t_0 &= \int_0^{a_0} \frac{da'}{\dot{a}'}. \end{aligned} \tag{26}$$

Therefore, from eq. (22), lookback time can be computed as

$$\begin{aligned} t_{lb} &= \int_{a_e}^{a_0} \frac{da}{a_0 H_0} \left[1 - \Omega_0^{(\mathrm{tot})} + \Omega_{\rho 0}(z+1)^{3w+1} + \Omega_{\Lambda 0}(z+1)^{-2}\right]^{-1/2} \\ &= H_0^{-1} \int_0^{z_e} dz'(z'+1)^{-2} \left[1 - \Omega_0^{(\mathrm{tot})} + \Omega_{\rho 0}(z'+1)^{3w+1} + \Omega_{\Lambda 0}(z'+1)^{-2}\right]^{-1/2}. \end{aligned} \tag{27}$$

For Chebyshev theorem of integration, we change the variable to $y = (1+z')^{-1} = a/a_0$ which is also known as the universe expansion function.

Therefore, from eq. (22) lookback time is given by the integral

$$t_{lb} = H_0^{-1} \int_{y_e}^{1} dy \left[1 - \Omega_0^{(\mathrm{tot})} + \Omega_{\rho 0}(y)^{-(3w+1)} + \Omega_{\Lambda 0}(y)^2\right]^{-1/2}. \tag{28}$$

The FLRW model can be reconstructed in $f(R,T)$ theory using an appropriate parameterization, and a variable cosmological parameter can be obtained. The density parameters in FLRW models are important cosmological parameters that can be used to study various cosmological models. The actual density (ρ_0) and the Hubble parameter (H_0) can be directly measured to determine the amount of mass in the universe.

By comparing ρ to the critical density, we can learn about the overall geometry of the universe and the fate of its expansion. By substituting different values of $\Omega_{\rho 0}$ and $\Omega_{\Lambda 0}$ we can analyze different models of the universe. Various models of the universe can vary also according to their nature of curvature, and for that, we have a specific set of equations which is evident from eq. (19) meaning

$$\begin{aligned} &\text{If } \Omega_\rho + \Omega_\Lambda = 1, \text{ meaning } k = 0 \text{ and it will be a flat universe;} \\ &\text{If } \Omega_\rho + \Omega_\Lambda < 1, \text{ meaning } k < 0 \text{ and it will be an open universe;} \\ &\text{If } \Omega_\rho + \Omega_\Lambda > 1, \text{ meaning } k > 0 \text{ and it will be a closed universe.} \end{aligned} \tag{29}$$

3.3 Analysis of FLRW Models based on Omega

We study various properties of the above-mentioned models of the universe, all of which are based on the FLRW Metric. The matter content of the respective universes is what determines the properties of the universe, in terms of structure, type of expansion, or even the fate of the universe. Specifically, we are looking at the values of $\Omega_{\Lambda 0}$ and $\Omega_{\rho 0}$ and determining these properties based on eq. (22), and also those depicted in eq. (29). From eq. (22), we can derive,

$$\left(\frac{\dot{a}}{a_0}\right)^2 = H_0^2\left[1 - \Omega_0^{(\text{tot})} + \Omega_{\rho 0}\left(\frac{a}{a_0}\right)^{-(3w+1)} + \Omega_{\Lambda 0}\left(\frac{a}{a_0}\right)^2\right] \tag{30}$$

Further on, we are considering dust-only models, meaning $w = 0$. We also substitute $\Omega_0^{(\text{tot})} = \Omega_{\rho 0} + \Omega_{\Lambda 0}$ as well as $y = \dfrac{a}{a_0}$ The equation can hence be written as

$$\left(\frac{\dot{a}}{a}\right)^2 \frac{1}{H_0^2} = \left(\frac{a_0}{a}\right)^2\left[1 - \Omega_{\rho 0} - \Omega_{\Lambda 0} + \Omega_{\rho 0}\left(\frac{a}{a_0}\right)^{-1} + \Omega_{\Lambda 0}\left(\frac{a}{a_0}\right)^2\right] \tag{31}$$

$$\implies \frac{H^2}{H_0^2} = \frac{1}{y^2} + \Omega_{\rho 0}\left(\frac{1}{y^3} - \frac{1}{y^2}\right) + \Omega_{\Lambda 0}\left(1 - \frac{1}{y^2}\right) \tag{32}$$

The scale factor a encodes data about the universe's structure and the type of expansion and it is dependent on the values of $\Omega_{\rho 0}$ and $\Omega_{\Lambda 0}$ when we consider equations for $\dot{a} = 0$ and $\ddot{a} = 0$, and we shall analyze various solutions. From Freidmann equation eq. (9), we can derive that

$$\frac{1}{H_0^2}\frac{\ddot{a}}{a} = \frac{-1}{2}\Omega_{\rho 0}\frac{1}{y^3} + \Omega_{\Lambda 0} = 0, \tag{33}$$

$$\implies \Omega_{\Lambda 0} = \frac{1}{2}\Omega_{\rho 0}\frac{1}{y^3}. \tag{34}$$

From eq. (32), if we consider $\dot{a} = 0$,

$$\implies \frac{1}{y^2} + \Omega_{\rho 0}\left(\frac{1}{y^3} - \frac{1}{y^2}\right) + \frac{1}{2}\Omega_{\rho 0}\frac{1}{y^3}\left(1 - \frac{1}{y^2}\right) = 0 \tag{35}$$

$$y^3 + \Omega_{\rho 0}(y^2 - y^3) + \frac{1}{2}\Omega_{\rho 0}(y^2 - 1) = 0 \tag{36}$$

Substituting $y = \dfrac{1}{2x}$, we gradually obtain

$$\begin{aligned}
&\implies 4x^2 + \Omega_{\rho 0}(8x^3 - 4x^2) + \frac{1}{2}\Omega_{\rho 0} x^3(1 - 4x^2) = 0, \\
&\implies 4x^3 - 3x + 1 - \frac{1}{\Omega_{\rho 0}} = 0, \\
&\therefore x^3 - \frac{3x}{4} + \frac{1}{4} - \frac{1}{4\Omega_{\rho 0}} = 0
\end{aligned} \tag{37}$$

The solution for this cubic equation can be expressed as

$$\begin{aligned}
&\text{If} \quad 0 < \Omega_{\rho 0} \leq \frac{1}{2}, \quad x = \cosh\left(\frac{1}{3}\cosh^{-1}\left(\frac{1}{\Omega_{\rho 0}} - 1\right)\right). \\
&\text{If} \quad \frac{1}{2} < \Omega_{\rho 0} \leq 1, \quad x = \cos\left(\frac{1}{3}\cos^{-1}\left(\frac{1}{\Omega_{\rho 0}} - 1\right)\right). \\
&\text{If} \quad \Omega_{\rho 0} > 1, \quad x = \cos\left(\frac{1}{3}\cos^{-1}\left(\frac{1}{\Omega_{\rho 0}} - 1\right) + \frac{4\pi}{3}\right)
\end{aligned} \tag{38}$$

With $\Omega_{\rho 0} = \frac{1}{2}, 1$ splitting the solutions, such that we get real positive values. If we consider the relation between $\Omega_{\rho 0}$ and $\Omega_{\Lambda 0}$ from eq. (34), we get the required critical functions for rebouncing (eq. (39)), and recollapsing models (eq. (40)) of the universe, which is depicted in Figures (3.1) and (3.2).

$$\begin{aligned}
&\text{When} \quad \Omega_{\Lambda 0} > 1 \quad \text{and if} \quad 0 \leq \Omega_{\rho 0} \leq \frac{1}{2}, \quad \Omega_{\Lambda 0} \geq 4\Omega_{\rho 0}\left[\cosh\left(\frac{1}{3}\cosh^{-1}\left(\frac{1}{\Omega_{\rho 0}} - 1\right)\right)\right]^3 \\
&\text{When} \quad \Omega_{\Lambda 0} > 1 \quad \text{and if} \quad \Omega_{\rho 0} > \frac{1}{2}, \quad \Omega_{\Lambda 0} \geq 4\Omega_{\rho 0}\left[\cos\left(\frac{1}{3}\cos^{-1}\left(\frac{1}{\Omega_{\rho 0}} - 1\right)\right)\right]^3
\end{aligned} \tag{39}$$

Otherwise,

$$\begin{aligned}
&\text{If} \quad 0 \leq \Omega_{\rho 0} \leq 1, \quad \Omega_{\Lambda 0} \leq 0. \\
&\text{If} \quad \Omega_{\rho 0} > 1, \quad \Omega_{\Lambda 0} \leq 4\Omega_{\rho 0}\left[\cos\left(\frac{1}{3}\cos^{-1}\left(\frac{1}{\Omega_{\rho 0}} - 1\right) + \frac{4\pi}{3}\right)\right]^3
\end{aligned} \tag{40}$$

This solution for eq. (37) can be derived using a trigonometric substitution.

$$4x^3 - 3x = \frac{1}{\Omega_{\rho 0}} - 1 \tag{41}$$

Consider $0 < \Omega_{\rho 0} \leq \frac{1}{2}$, which implies $\frac{1}{\Omega_{\rho 0}} - 1 > 0$, and we substitute

$$\cosh 3\beta = \frac{1}{\Omega_{\rho 0}} - 1 = 4\cosh^3\beta - 3\cosh\beta \quad \text{where} \quad x = \cosh\beta \tag{42}$$

$$\begin{aligned} \implies \beta &= \frac{1}{3}\cosh^{-1}\left(\frac{1}{\Omega_{\rho 0}} - 1\right) \\ \therefore \Omega_{\Lambda 0} &= 4\Omega_{\rho 0}\left[\cosh\left(\frac{1}{3}\cosh^{-1}\left(\frac{1}{\Omega_{\rho 0}} - 1\right)\right)\right]^3 \end{aligned} \tag{43}$$

Now consider $\frac{1}{2} < \Omega_{\rho 0} \leq 1$, which implies $\frac{1}{\Omega_{\rho 0}} - 1 > 0$, and we substitute

$$\cos 3\beta = \frac{1}{\Omega_{\rho 0}} - 1 = 4\cos^3\beta - 3\cos\beta \quad \text{where} \quad x = \cos\beta \tag{44}$$

$$\begin{aligned} \implies \beta &= \frac{1}{3}\cos^{-1}\left(\frac{1}{\Omega_{\rho 0}} - 1\right) \\ \therefore \Omega_{\Lambda 0} &= 4\Omega_{\rho 0}\left[\cos\left(\frac{1}{3}\cos^{-1}\left(\frac{1}{\Omega_{\rho 0}} - 1\right)\right)\right]^3 \end{aligned} \tag{45}$$

Those equations, namely eqs. (39) and (40) are important to construct the diagram in Fig. 3.1 (and in detail also in Fig. 3.2), which illustrates the various scenarios depending on the values of $\Omega_{\rho 0}$ and $\Omega_{\Lambda 0}$. Both rebouncing and recollapsing cosmological models challenge the conventional understanding of the universe's evolution based on the Big Bang theory and cosmic inflation. They offer alternative explanations for the observed large-scale structure of the universe, the abundance of cosmic microwave background radiation, and other cosmological phenomena.

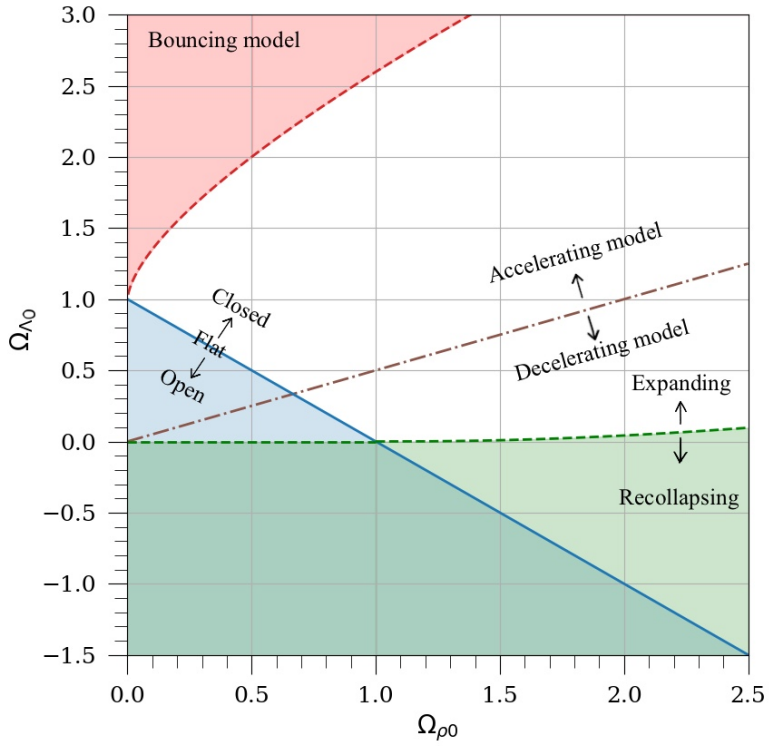

Figure 3.1: Comparative study of evolution of $\Omega_{\lambda 0}$ vs $\Omega_{\rho 0}$ for different FLRW models of the universe. Depending on the values of $\Omega_{\lambda 0}$ and $\Omega_{\rho 0}$ the universe in consideration can be (re-)bouncing model or eternally inflating. The structure of the universe can be closed, flat, or open. It can also be categorized into expanding and recollapsing models. The expansion itself of the universe can be accelerating or decelerating according to the matter content of the universe or the model under study.

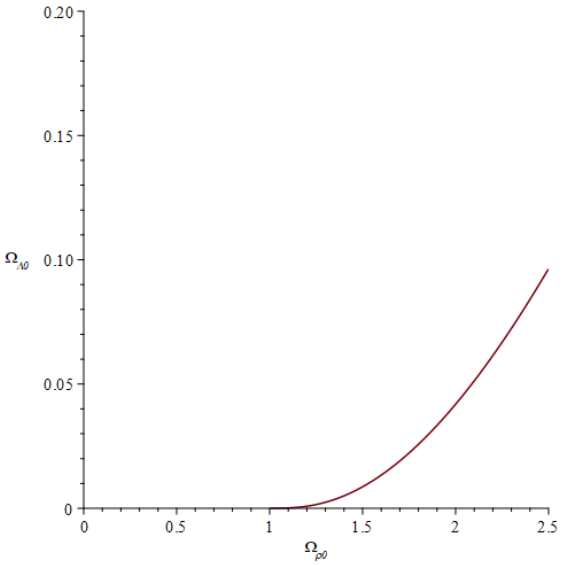

Figure 3.2: A magnified view for the boundary between Expanding vs Recollapsing models

Various well-known FLRW models are discussed in the following subsections.

3.3.1 Einstein de Sitter Model

The Einstein de Sitter Model is a well-known standard model with standard results with which we compare all other models in this work and it is characterized by

$$k = 0, \quad \Omega_{\rho 0} = 1, \quad \Omega_{\Lambda 0} = 0. \tag{46}$$

The content of the universe is only dust, no radiation exists as well as no dark matter. The universe also has zero curvature and is a flat one.

Therefore,

$$a(t) = a_0 \left(\frac{3}{2} H_0 t\right)^{2/3} \quad H(t) = \frac{2}{3t} \tag{47}$$

The energy density of matter can also be derived as

$$\rho_{m0} = \frac{3H_0^2}{8\pi G}, \quad \rho_m(t) = \rho_{m0} \left(\frac{t_0}{t}\right)^2. \tag{48}$$

These results can be substituted into eq. (22) to get

$$\dot{a} = a_0 H_0 (z+1)^{1/2}. \tag{49}$$

Eqs. (27,28) can also be substituted to get lookback times for Einstein de Sitter universe

$$H_0 t_{lb} = \frac{2}{3}\left[1 - \frac{1}{(1+z_e)^{3/2}}\right], \quad H_0 t_{lb} = \frac{2}{3}(1 - y_e^{3/2}). \tag{50}$$

3.3.2 Lambda CDM Model

The ΛCDM cosmological model also known as the Big Chill model is also known as the benchmark model. The ΛCDM model is the standard model of the universe, which is based on the Big Bang theory and includes both dark matter and dark energy. It is called ΛCDM because it includes a cosmological constant (Λ) and cold dark matter (CDM).

According to the ΛCDM model, the cosmos is assumed to be homogenous and isotropic on large scales, meaning that it appears the same from all angles and locations. Observations of the cosmic microwave background radiation, which is the lingering heat from the Big Bang, lend credence to this hypothesis. The model also makes the assumption that the universe is flat, in which case its geometry is Euclidean. Observations of the universe's large-scale structure lend credence to this hypothesis.

The ΛCDM model predicts that about 5% of the universe is made up of ordinary matter, such as protons and neutrons, while about 27% is made up of dark matter, which interacts only through gravity. The remaining 68% is made up of dark energy, which is responsible for the observed acceleration of the universe's expansion. In the ΛCDM model, the total density parameter Ω_{tot} is equal to 1, which means that the universe is flat. The matter density parameter $\Omega_{\rho 0}$ is about 0.31, Ω_{Λ_0} is 0.69 (we follow the values given in [4]). The inclusion of dark energy in the Lambda-CDM model suggests that the universe will expand forever.

While the ΛCDM model has strong observational support, it still has some unresolved issues, such as the nature of dark matter and dark energy. It is possible that these issues will be resolved by future observations or by modifications to the model, such as the inclusion of a scalar field that drives the acceleration of the universe.

The ΛCDM model or the benchmark model is characterized by

$$k = 0, \quad \Omega_{\rho 0} = 0.31, \quad \Omega_{\Lambda 0} = 0.69. \tag{51}$$

Eq. (22) can be substituted to get (considering dust only),

$$\dot{a} = a_0 H_0 \sqrt{0.31(z+1) + 0.69(z+1)^{-2}} \tag{52}$$

Similarly eqs. (27, 28) can also be substituted to get lookback times for the ΛCDM model

$$H_0 t_{lb} = \int_0^{z_e} dz'(z'+1)^2 \left[0.31(z'+1) + \frac{0.69}{(z'+1)^2}\right]^{-1/2}, \quad H_0 t_{lb} = \int_{y_e}^{1} dy \left[\frac{0.31}{y} + 0.69y^2\right]^{-1/2} \tag{53}$$

3.3.3 Big Crunch Model

The Big Crunch is a theoretical model in FLRW (Friedmann-Lemaître-Robertson-Walker) cosmology that suggests a possible fate for the universe. It proposes that the expansion of the universe will eventually reverse, leading to a contraction of spacetime, ultimately resulting in a cosmic collapse known as the Big Crunch.

In FLRW cosmology, the evolution of the universe is described by the Friedmann equations, which relate the expansion rate of the universe to its matter and energy content. The Friedmann equations take into account the density of matter, radiation, dark energy, and the curvature of spacetime.

The Big Crunch scenario arises when the total density of matter and energy in the universe exceeds a critical value. This critical density, determines the fate of the universe. If the total density is less than the critical density, the universe will continue to expand indefinitely, with the expansion rate gradually decreasing over time. This scenario is known as a ”open universe” or ”unbounded universe.”

However, if the total density equals or exceeds the critical density, the universe will eventually reach a point where the expansion stops and is reversed. At this stage, gravity becomes the dominant force, causing the universe to contract. This contraction continues until all matter and energy are concentrated in a singularity, resulting in a state of extreme density and temperature. This is what is referred to as the Big Crunch. During the contraction phase of the Big Crunch, the scale factor of the universe, denoted by ’a(t)’, decreases with time. Distances between objects decrease as the universe collapses, and the curvature of spacetime becomes more pronounced. As the contraction progresses, the density and temperature of the universe increase enormously.

The consequences of the Big Crunch model are significant. If the universe does undergo a Big Crunch, it would mark the end of the current cycle of expansion and contraction. It would also imply a highly compressed and high-energy state, potentially leading to the formation of a singularity, similar to the initial state of the universe in the Big Bang model The Big Crunch Model for the FLRW Metric typically has a negative cosmological constant or matter significantly dominating over dark energy (see Fig. 3.1). For our model we took the case, whose dark energy density parameter is equal in magnitude to the matter content of the universe and hence is an open universe (corresponding to the green bottom region in Fig. 3.1):

$$k = -1, \quad \Omega_{\rho 0} = 0.31, \quad \Omega_{\Lambda 0} = -0.31. \tag{54}$$

From eq. (22) we can see that(considering dust only)

$$\dot{a} = a_0 H_0 \sqrt{1 + 0.31(z+1) - 0.31(z+1)^{-2}} \tag{55}$$

Similarly, from eqs. (27, 28) we can see that, for the Big Crunch Universe Model, lookback times can be derived as

$$H_0 t_{lb} = \int_0^{z_e} dz'(z'+1)^2 \left[1 + 0.31(z'+1) + \frac{0.31}{(z'+1)^2}\right]^{-1/2}, \quad H_0 t_{lb} = \int_{y_e}^{1} dy \left[1 + \frac{0.31}{y} - 0.31y^2\right]^{-1/2}. \tag{56}$$

3.3.4 Empty Universe Model

The Empty Universe model is a cosmological model that assumes that the universe contains no matter or radiation, and is therefore completely empty. It is also known as the vacuum universe or the zero-energy universe. This model is based on the idea that the total energy of the universe is exactly zero, which means that the positive energy of matter is balanced out by the negative energy of gravity.

One of the key predictions of this model is that the universe would expand forever, with no deceleration due to the gravitational pull of matter. This is because in an empty

universe, there is no matter to exert a gravitational force on the expansion.

However, the Empty Universe model is not consistent with current observations, which show that the universe is not empty but contains a significant amount of matter and radiation. In fact, the existence of dark matter and dark energy suggests that the universe has a positive energy density, rather than a zero energy density as predicted by the Empty Universe model. Therefore, this model is not considered to be a viable explanation for the observed properties of the universe. And it is also evident that this universe is an open one:

$$k = -1, \quad \Omega_{\rho 0} = 0, \quad \Omega_{\Lambda 0} = 0. \tag{57}$$

From eq. (22) we can see that

$$\dot{a} = a_0 H_0, \quad a = a_0 H_0 t. \tag{58}$$

Lookback times for Empty Universe Model can be derived using eqs. (27, 28) which give us

$$H_0 t_{lb} = 1 - \frac{1}{z_e + 1}, \quad H_0 t_{lb} = 1 - y_e \tag{59}$$

3.3.5 Loitering Universe

The Loitering Universe model is a cosmological model that suggests that the universe is expanding at a rate that is just enough to counteract the gravitational attraction between all of its matter. In this model, the universe will continue to expand forever but will do so at an increasingly slower rate, eventually coming to a complete stop and reaching a state of infinite size.

One of the major limitations of the Loitering Universe model is that it requires a very specific balance between the expansion rate of the universe and the gravitational attraction between all of its matter. This balance is difficult to explain, and the model has not been able to explain certain observed properties of the universe, such as Cosmic Microwave Background Radiation. Overall, while the Loitering Universe model is an interesting

concept, it is not currently considered a viable explanation for the observed properties of the universe. Loitering universe predicts a closed Universe model, which predicts that the universe has positive curvature, and that parallel lines will eventually converge at a point. For our particular numerical model we have taken

$$k = 1, \quad \Omega_{\rho 0} = 0.31, \quad \Omega_{\Lambda 0} = 1.7289. \tag{60}$$

Eq. (22) gives us (considering dust only)

$$\dot{a} = a_0 H_0 \sqrt{-0.9599 + 0.31(z+1) + 1.7289(z+1)^{-2}} \tag{61}$$

Similarly eqs. (27, 28) imply that for the Loitering Universe, the lookback times can be derived as

$$\begin{aligned} H_0 t_{lb} &= \int_0^{z_e} dz'(z'+1)^2 \left[-0.9599 + 0.31(z'+1) + \frac{1.7289}{(z'+1)^2} \right]^{-1/2}, \\ H_0 t_{lb} &= \int_{y_e}^{1} dy \left[-0.9599 + \frac{0.31}{y} + 1.7289(y)^2 \right]^{-1/2}. \end{aligned} \tag{62}$$

3.3.6 Big Bounce Universe

According to the Big Bounce Universe Model, the universe did not begin with a Big Bang but rather by contracting from a vast volume and then expanding again. It is related to cyclic models in some cases when the universe goes through cycles of expansion and contraction. Such a Big Bounce concept is derived from the Loop Quantum Gravity theory, which postulates that spacetime is quantized and that there is a minimum length scale. This hypothesis contends that because singularities defy the laws of physics, the universe could not have begun with one. Instead, the contraction would have been prevented by quantum phenomena, and the cosmos would have recovered from it.

The Big Bounce Universe Model has gained popularity in recent years as an alternative to the Big Bang theory, which so far does not fully explain the very origin of the universe. However, there is currently no direct evidence to support the Big Bounce theory, and it remains a subject of debate among cosmologists.

The curvature of the Big Bounce Universe is still a subject of debate among cosmologists. Some suggest that the universe may have a flat curvature, while others propose that it may be negatively curved. The curvature of the universe is determined by its density and expansion rate. If the density is greater than the critical density, the universe has a positive curvature and is closed. If the density is less than the critical density, the universe has a negative curvature and is open. If the density is exactly equal to the critical density, the universe has a flat curvature. In classical general relativity and in accordance with Fig. 3.1, here we are considering a closed universe with positive curvature (belongin to the top-left red region in Fig. 3.1):

$$k = 1, \quad \Omega_{\rho 0} = 0.31, \quad \Omega_{\Lambda 0} = 1.8. \tag{63}$$

Eq. (22) can be used to derive (considering dust only)

$$\dot{a} = a_0 H_0 \sqrt{0.31(z+1) + 1.8(z+1)^{-2}} \tag{64}$$

Eqs. (27, 28) can be used to derive lookback times for Big Bounce Universe

$$H_0 t_{lb} = \int_0^{z_e} dz'(z'+1)^2 \left[0.31(z'+1) + \frac{1.8}{(z'+1)^2}\right]^{-1/2}, \quad H_0 t_{lb} = \int_{y_e}^{1} dy \left[\frac{0.31}{y} + 1.8(y)^2\right]^{-1/2}. \tag{65}$$

3.3.7 Pure Lambda/ de Sitter Universe

In its future evolution, the Pure Lambda model or the de Sitter Universe is a close relative of the ΛCDM model, which is the current standard model of cosmology. The de Sitter Universe, on the other hand, is a model that assumes the universe is empty and consists only of vacuum energy (which is suppose to dominate in our universe now as well). In this model, the universe is also flat and infinite, but its expansion is accelerating due to the repulsive force of vacuum energy.

Both models have their limitations. The Pure Lambda model requires the existence of dark matter and dark energy, which have not been directly observed, and the nature of

which remains a mystery. The de Sitter Universe model also requires the existence of vacuum energy, which is difficult to reconcile with quantum mechanics.

Despite their limitations, both models have been used to make successful predictions about the large-scale structure of the universe, such as the cosmic microwave background radiation and the distribution of galaxies. However, there is currently no direct evidence to support either model, and they remain subjects of debate among cosmologists

$$k = 0, \quad \Omega_{\rho 0} = 0, \quad \Omega_{\Lambda 0} = 1. \tag{66}$$

$$\dot{a} = a_0 H_0 (z+1)^{-1}, \quad \implies a = a_0 e^{H_0 t}. \tag{67}$$

Eqs. (27, 28) can be used to derive the lookback time for a Pure Lambda/ de Sitter Universe

$$H_0 t_{lb} = \int_0^{z_e} dz' (z'+1)^{-2} \left[\Omega_{\Lambda 0}(z'+1)^{-2}\right]^{-1/2}, \quad H_0 t_{lb} = \int_{y_e}^{1} dy \left[\Omega_{\Lambda 0}(y)^2.\right]^{-1/2} \tag{68}$$

$$H_0 t_{lb} = \ln(1+z_e), \quad H_0 t_{lb} = -\ln y_e. \tag{69}$$

3.4 Various lookback times for FLRW Models

For the different models in consideration, lookback times have been graphed with respect redshift z due to the expansion in the given FLRW models. As the inverse Hubble constant has a dimension of time, it is convenient to introduce a Hubble time as a basic time scale. Lookback time can be scaled as $H_0 t_{lb} = t_{lb}/t_H$ for convenience. For a particular value of H_0 it can be easily converted to time in seconds or years; e.g. with $H_0 = 70\,\mathrm{km/s/Mpc}$ as per eq. (146) we get

$$\text{Hubble Time} \quad t_H \approx \frac{1}{H_0} \approx 13.978 \times 10^9 \text{years}. \tag{70}$$

From the graphs depicted below we can see that lookback time relies heavily on the matter content, giving rise to peculiar graphs for models such as the loitering universe

and rebouncing model, whereas most other models have almost a generic structure. It is also worth noting that even the empty universe and the pure Lambda universe have almost generic graphs. In rebouncing model, the graph clearly depicts the increase as well as the decrease of redshift, indicating a blue shift as the universe was collapsing.

The generic models however have somewhat similar shapes. At low redshifts (near $z = 0$), the lookback time will be relatively small, corresponding to a more recent time in the universe's history, closer to our present epoch. As redshift increases, the lookback time will progressively grow, indicating the increasing age of the observed objects. The slope of the graph might become steeper initially. At higher redshifts, approaching the early universe (large z values), the lookback time will become significantly larger, representing light emitted from distant and much earlier cosmic epochs.

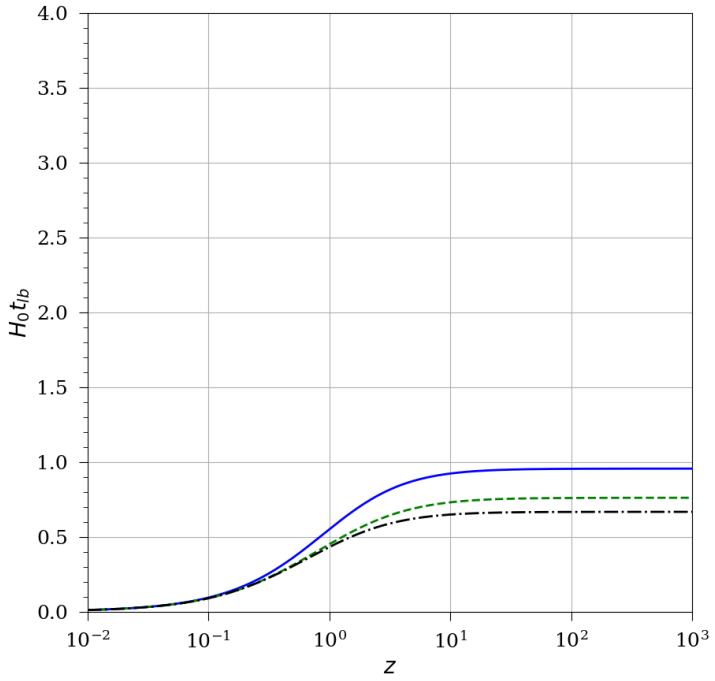

Figure 3.3: Lookback time (scaled) $H_0 t_{lb}$ versus Redshift factor z for the given FLRW Models. Einstein-de Sitter model (black dash-dot) (50), Benchmark model (solid blue line) (53), Big Crunch model (green short dash) (56)

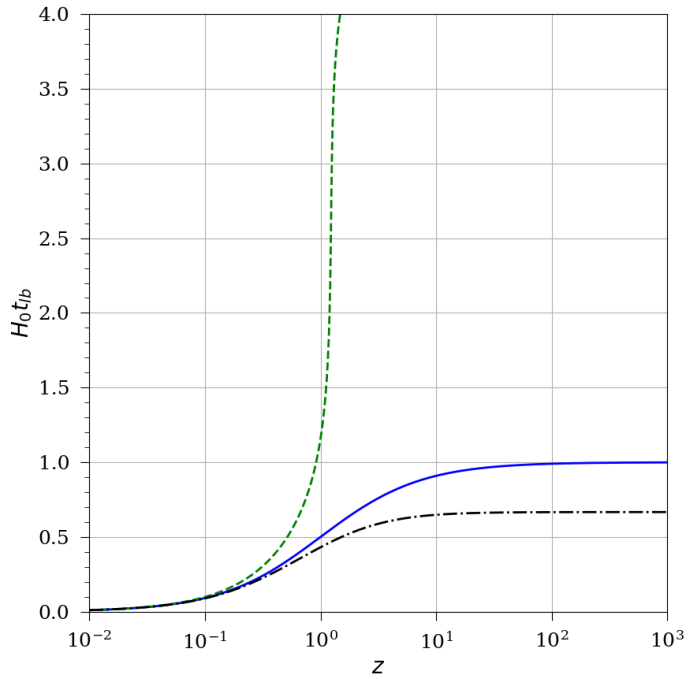

Figure 3.4: Lookback time (scaled) $H_0 t_{lb}$ versus Redshift factor z for the given FLRW Models. Einstein-de Sitter model (black dash-dot) (50), Loitering Universe (solid blue line) (62), Empty Universe (green short dash) (59).

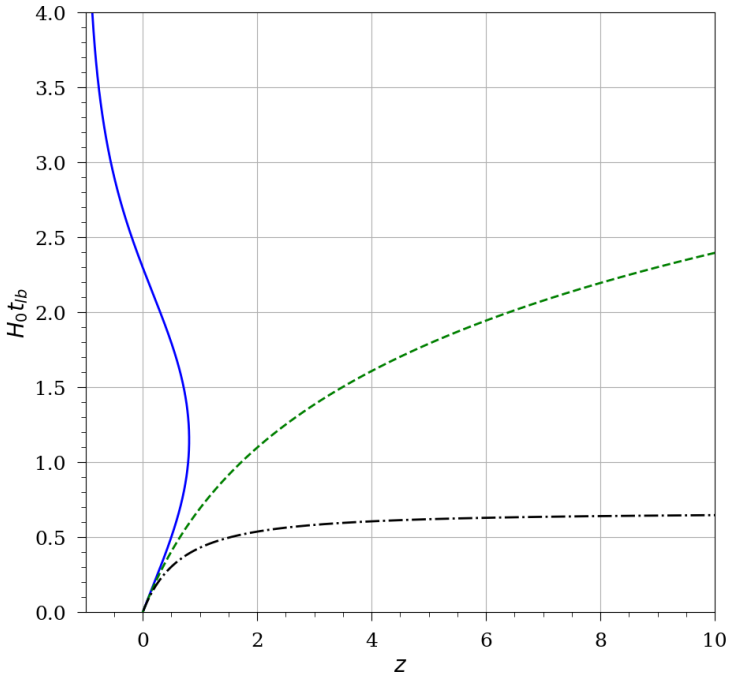

Figure 3.5: Lookback time (scaled) $H_0 t_{lb}$ versus Redshift factor z for the given FLRW Models. Einstein-de Sitter model (black dash-dot) (50), Rebouncing Universe (solid blue line) (65), Pure Lambda Universe (green short dash) (69).

Chapter 4

Horizons

It is more challenging to apply the idea of a gravitational radius in cosmology than, for instance, to a compact star. It is simple to grasp how the gravitational influence of the well-defined mass warped the surrounding spacetime when the matter is scattered within a constrained (more or less) spherical zone surrounded by a vacuum. When a star's radius is small enough to enable escape velocity to be equal to or greater than the speed of light, c, it is said to have an apparent horizon. These settings have what are known as event horizons yet appear to have gravitational horizons, and these objects are frequently referred to by both names. This is because the Schwarzschild and Kerr metrics used to specify the spacetime surrounding those blackholes are time-independent.

We'll find that the "gravitational radius", R_h, of this horizon is the same as the sphere's far more well-known radius. In fact, the existence of a gravitational horizon is what makes a Hubble radius possible. The latter exists solely as the former's manifestation in the world. It is reliant on the equation of state of the cosmic fluid and is time-dependent rather than static like its equivalent in the Schwarzschild and Kerr metrics. It may or may not eventually transform into an event horizon in the asymptotic future. A Newtonian theorem relating to spherical mass distributions has a relativistic generalization known as the Birkhoff theorem.It asserts that the Schwarzschild metric may be used to characterise the surrounding spacetime for any isotropic, spherically symmetric distribution of mass energy, whether static or time-dependent. The Birkhoff theorem's corollary asserts that, for an isotropic universe, the mass-energy content inside a sphere with a radius

of R determines the spacetime curvature at that radius; the rest of the universe, due to spherical symmetry, has no bearing on the metric at that radius. Because the origin could be anywhere in the cosmos, a radius R for one observer might differ from a radius R' for another. The result is that in this situation, only relative spacetime curvature matters.

Which also depicts, depending merely on the amount of mass-energy that exists between them, any two locations in a medium with a non-zero energy density ρ experience a net acceleration (or deceleration) towards (or away from) one another. The Universe cannot be static because, despite the possibility that it is infinite, local motions depend dynamically only on local densities. Imagine that the observer has now increased the range of his vision. A gravitational horizon will eventually be created by his expanding sphere of radius R at the specified density ρ, which is equal to R_h for the FLRW metric.

4.1 Horizon radius in FLRW metric

The scale factor $a(t)$ in the metric given by eq. (4), is transformed using the relation

$$a(t) = e^{f(t)} \tag{71}$$

where $f(t)$ is itself a function only of cosmic time t.
With current observational values indicating a flat universe, where $k = 0$, the metric can be written as

$$ds^2 = c^2dt^2 - e^{2f(t)}\left[dr^2 + r^2\left(d\theta^2 + \sin^2\theta d\phi^2\right)\right] \tag{72}$$

From Eqs. (7) and (71), we can see that

$$r = Re^{-f} \tag{73}$$

which implies,

$$\begin{aligned} dr &= e^{-f}[dR - R\dot{f}dt] \\ dr^2 &= e^{-2f}\left[dR^2 + (R\dot{f})^2dt^2 - 2(R\dot{f})dtdR\right] \end{aligned} \tag{74}$$

which can also be rearranged as

$$dr^2 = e^{-2f}\left[dR^2 + \left(\frac{R\dot{f}}{c}\right)^2 c^2dt^2 - 2\left(\frac{R\dot{f}}{c}\right)cdtdR\right] \tag{75}$$

Substituting in eq. (72),

$$ds^2 = c^2dt^2 - \left[dR^2 + \left(\frac{R\dot{f}}{c}\right)^2 c^2dt^2 - 2\left(\frac{R\dot{f}}{c}\right)cdtdR + R^2\left(d\theta^2 + \sin^2\theta d\phi^2\right)\right] \tag{76}$$

Rearranging the terms, we can now write the metric as

$$ds^2 = \left[1 - \left(\frac{R\dot{f}}{c}\right)^2\right]c^2dt^2 + 2\left(\frac{R\dot{f}}{c}\right)cdtdR - dR^2 - R^2d\Omega^2 \tag{77}$$

where $d\Omega^2 = d\theta^2 + \sin^2\theta d\phi^2$.

We define the quantity

$$\Phi \equiv 1 - \left(\frac{R\dot{f}}{c}\right)^2 \tag{78}$$

which appears frequently in the metric coefficients. So that the metric in (77) can be written as

$$ds^2 = \Phi c^2dt^2 + 2\Phi\left(\frac{R\dot{f}}{c}\right)\Phi^{-1}cdtdR - \left[1 - \left(\frac{R\dot{f}}{c}\right)^2\right]\Phi^{-1}dR^2 - R^2d\Omega^2 \tag{79}$$

Completing squares, we get

$$ds^2 = \Phi\left[cdt + \left(\frac{R\dot{f}}{c}\right)\Phi^{-1}dR\right]^2 - \Phi^{-1}dR^2 - R^2d\Omega^2 \tag{80}$$

Rewriting in standard form, we get

$$ds^2 = \Phi\left[1 + \left(\frac{R\dot{f}}{c}\right)\Phi^{-1}\frac{\dot{R}}{c}\right]^2 c^2dt^2 - \Phi^{-1}dR^2 - R^2d\Omega^2 \tag{81}$$

In a cosmological context, the functions of time t are $\dot{R}$ and $\dot{f}$. In other words, the Universe is expanding, as indicated by the FLRW metric when expressed in terms of R and t. The factor can be explained physically using Birkhoff's theorem and its corollary,

which, as we've seen, state that measurements made by an observer at a distance R from his location (at the origin of his coordinates) are unaffected by the mass-energy content of the Universe outside to the shell at R, can be used to find a physical interpretation of the factor $\frac{\dot{f}}{c}$ and, in fact, the function Φ itself. The threshold distance scale is reached when $R \to R_h$, where

$$R_h = c/\dot{f} \tag{82}$$

This equation is also self-consistent with the fact that, in this gauge, apparent horizons are located by the constraint $g^{RR} = 0$, which gives us the condition $\Phi = 0$. On comparing the R_h we have derived here with the usual Schwarzschild horizon radius

$$R_h = \frac{2GM}{c^2} \tag{83}$$

where M is the proper mass contained within a sphere of proper radius R_h, and can also be written as

$$M \equiv \frac{4\pi}{3} R_h^3 \rho \tag{84}$$

This mass is referred to as the Misner-Sharp mass, and on occasion as the Misner-Sharp-Hernandez mass [19]. These statements are based on Misner and Sharp's groundbreaking research on the issue of spherical collapse in general relativity. A sphere with this radius is not necessarily an event horizon because, unlike the Schwarzschild and Kerr metrics, the cosmological R_h may fluctuate over time. Depending on the characteristics of the cosmic fluid, it might develop into one in the asymptotic future. In either case, a gravitational horizon defined by the constant R_h makes a distinction between null geodesics moving in either our direction or away from us at any cosmic time t.

From Eqs. (83) and (84), it is clearly visible that

$$R_h^2 = \frac{3c^2}{8\pi G\rho} \tag{85}$$

Comparing this result with Friedmann equations (8), and considering a flat universe

$(k = 0)$, we get

$$R_h = \frac{c}{H} = \frac{ca}{\dot{a}} \tag{86}$$

That is, $R_h = c/\dot{f}$.

Equation (86) is fully self-consistent with its well-known equivalent in the study of apparent horizons in cosmology. Thus, the FLRW metric equation (81) can alternatively be expressed in the following way:

$$ds^2 = \Phi \left[1 + \left(\frac{R}{R_h}\right) \Phi^{-1} \frac{1}{c} \dot{R}\right]^2 c^2 dt^2 - \Phi^{-1} dR^2 - R^2 d\Omega^2, \tag{87}$$

in which the function

$$\Phi \equiv 1 - \left(\frac{R}{R_h}\right)^2 \tag{88}$$

shows how the proximity of the appropriate distance R to the gravitational radius R_h affects the coefficients $g_t t$ and $g_R R$. We can already use this metric to analyze how the cosmic spacetime behaves at any radius R. The de Sitter metric is one of the few examples where it may be desirable to "complete" the transformation by including a new time coordinate T, so that

$$\Phi^{-1/2} \frac{cdT}{\beta(t, R)} \equiv \Phi^{1/2} cdt + \left(\frac{R}{R_\mathrm{h}}\right) \Phi^{-1/2} dR \tag{89}$$

where $\beta(t, R)$ is an integrating factor selected to guarantee that dT is an exact differential. There could be an infinite number of solutions to the equation $\beta(t, R)$, but only one of them completely diagonalizes the metric and is dimensionless, ensuring that T has time dimensions. This substitution, however,

$$ds^2 = \Phi^{-1} \frac{c^2 dT^2}{\beta^2(t, R)} - \Phi^{-1} dR^2 - R^2 d\Omega^2 \tag{90}$$

However T must satisfy the following condition in order for dT to be an exact differential,

$$\frac{\partial^2 T}{\partial R \partial t} = \frac{\partial^2 T}{\partial t \partial R} \tag{91}$$

Meaning $\beta(t, R)$ must be a solution to the equation

$$\frac{\partial}{\partial R}[\Phi\beta(t,R)] = \frac{\partial}{\partial t}\left[\left(\frac{R}{cR_{\mathrm{h}}}\right)\beta(t,R)\right] \tag{92}$$

However, as we will see in a moment, the coordinate T has only a limited range of applications because it is extremely uncommon to be able to integrate dT from the time of the big bang at $t = 0$ to the present.

4.2 Geodesics in FLRW Models

From eq. (7), and Weyl's postulate, we know that for comoving observers, worldlines are dictated by

$$\dot{R}(t) = \dot{a}r \tag{93}$$

which can also be used to reach Hubbles' law again, since

$$\dot{R} = \frac{\dot{a}}{a}R \equiv HR = \frac{cR}{R_h} \tag{94}$$

For a particle geodesic, the coefficient g_{tt} is given by

$$\begin{aligned} g_{tt} &= \Phi\left[1 + \left(\frac{R}{R_h}\right)\Phi^{-1}\right]^2 \\ \implies g_{tt} &= \Phi^{-1} \end{aligned} \tag{95}$$

Thus, the FLRW metric for a particle worldline, expressed in terms of cosmic time t and proper radius R can be written as

$$ds^2 = \Phi^{-1}c^2dt^2 - \Phi^{-1}dR^2 - R^2d\Omega^2 \tag{96}$$

But from eq. (93), we know that

$$dR = c\left(\frac{R}{R_h}\right)dt \tag{97}$$

Thus reducing eq. (96) to the final form,

$$ds^2 = c^2dt^2 - R^2d\Omega^2 \tag{98}$$

To describe a particle moving radially with Hubble flow (i.e., with $\dot{R} = HR$ and $d\Omega = 0$), is therefore

$$ds = cdt. \tag{99}$$

This exhibits behavior that is consistent with how our coordinates were originally defined. In particular, the cosmic time t, which is unaffected by the location R, is the correct time as measured in the comoving frame everywhere in the universe. As free-falling observers in this frame, our clocks must accurately display local time without interference from any external gravitational forces.

The situation, however, fundamentally alters when we examine how the metric behaves with respect to the observer when applied to a fixed radius $R = R_0$. Those familiar with the Schwarzschild and Kerr metrics in black-hole systems compare this position to that of an observer maintaining a stable radius with respect to the central source of gravity. In contrast to the previous example, where R was connected to particles (such as galaxies) expanding with the Hubble flow, we now set the distance to R_0 and instead consider particles traveling through this region. We expect that gravitational influences will manifest themselves in the metric by analogy with the Schwarzschild situation since we are no longer measuring from a free-falling perspective.

Returning to eq. (87), we have in this case $dR = 0$, so that

$$ds^2 = \Phi_0 c^2dt^2 - R_0^2d\Omega^2, \tag{100}$$

and the metric has the following form if we once more insist on purely radial motion (with $dOmega2 = 0$).

$$ds^2 = \Phi_0 c^2dt^2 \tag{101}$$

where now $\Phi_0 \equiv 1 - (R_0/R_\mathrm{h})^2$.

This formula replicates the effect that one would have anticipated, where the passing of time at a fixed proper radius R_0 is no longer the proper time in a local free-falling frame. It is similar to Schwarzschild and Kerr. The gravitational horizon features are typically linked to the Schwarzschild radius in compact objects, but for any finite interval, $ds, dt \to \infty$ as $R_0 \to R_h$ is another option.

Even though the scenario for null geodesics is slightly different, it is still entirely consistent with the more well-known behavior observed in black-hole spacetimes. By examining the FLRW metric in eq. (4), it is simple to verify that $dotr$ cannot be zero for a light beam. The null condition (i.e., $ds = 0$), a radial path, and, as always, a flat universe with $k = 0$ lead to the expression.

$$cdt = \pm adr \tag{102}$$

Clearly indicating that along an inwardly propagating radial null geodesic, this equation gives the specific path followed by the null geodesic in spacetime. The solution depends on the specific geometry and distribution of mass and energy in the spacetime under consideration, vis-a-vis the scale factor.

$$\dot{r} = -\frac{c}{a} \tag{103}$$

Therefore, the time interval dt corresponding to any measurable (non-zero) value of ds must go to infinity as $R \to R_h$ if a measurement were to be taken at a certain distance R from us. This phenomenon is known as the divergent gravitational redshift perceived by a stationary observer outside the event horizon in terms of black-hole physics. Despite the fact that, as we shall see, in some situations, R_h is beyond the distance ct_0 light has traveled since the Big Bang and is hence not an observable quantity, this result holds for all cosmologies. However, the elements of the universe that directly determine the value of w, the function f, and the radius of the horizon R_h do vary from one instance to the next.

But from eqs. (86) and (8), we can clearly see that, for a flat universe with $k = 0$,

$$\frac{d}{dt}(R_h) = \frac{d}{dt}\left(\frac{ca}{\dot{a}}\right) = c\left(\frac{\dot{a}^2 - a\ddot{a}}{\dot{a}^2}\right) = c\left(1 - \left(\frac{a}{\dot{a}}\right)^2\left(\frac{\ddot{a}}{a}\right)\right) \tag{104}$$

$$\implies \dot{R}_h = c\left(1 - \frac{-\frac{4\pi G}{3c^2}\rho(1+3w)}{\frac{8\pi G}{3c^2}\rho}\right) = c\left(1 + \frac{1+3w}{2}\right) \tag{105}$$

$$\therefore \dot{R}_h = \frac{3}{2}(1+w)c \tag{106}$$

Therefore, for any cosmological system with $w > -1$, R_h is an increasing function of cosmic time t. Only the de Sitter universe, where $w = -1$ and ρ is the cosmological constant, has this stable value. Additionally, a boundary is evident at $w = -1/3$. Since light would have traveled a distance ct_0 more than $R_h\,(t_0)$ since the big bang, our universe would be defined by this horizon when $w - 1/3$ and R_h rises slower than lightspeed. However, when $w > -1/3$, R_h is always bigger than ct, and our observational limit would then be determined by the length of time it takes for light to travel through space (ct_0).

4.3 Study of Horizons for various FLRW Models

We look at specific FLRW universes only with zero curvature. The concept of a horizon sphere, in this work is only associated with a flat universe. FLRW models with positive or negative curvatures are more intricate to visualize but mathematically not impossible.

4.3.1 Apparent Horizon for Einstein de Sitter Universe

As we recall from eq. (47), considering present-day value of the scale factor scaled to $a_0 = 1$, we get

$$a(t) = \frac{3}{2}H_0 t \quad H(t) = \frac{2}{3t} \tag{107}$$

The metric of spacetime can be written as

$$ds^2 = c^2dt^2 - \left(\frac{3}{2}H_0 t\right)^2\left[dr^2 + r^2 d\Omega^2\right] \tag{108}$$

Therefore, since $a = e^{f(t)}$,

$$f(t) = \ln[a(t)] = \frac{2}{3} \ln\left(\frac{3}{2} H_0 t\right) \tag{109}$$

Meaning,

$$\dot{f} = \frac{2}{3t} \tag{110}$$

And the radius of the apparent horizon

$$R_h = (3/2)ct \quad \dot{R}_h = (3/2)c \tag{111}$$

Thereby, the metric is written as

$$ds^2 = \Phi \left[cdt + \left(\frac{R}{3ct/2}\right) \Phi^{-1} dR\right]^2 - \Phi^{-1} dR^2 - R^2 d\Omega^2 \tag{112}$$

where

$$\Phi = 1 - \left(\frac{R}{3ct/2}\right)^2 \tag{113}$$

Calculating the dimensionless integrating factor $\beta(t, R)$

$$\beta(t, R) = \sqrt{1 + \frac{1}{2}\left(\frac{R}{R_\mathrm{h}}\right)^2} \tag{114}$$

Thus, in terms of R and T,

$$ds^2 = \Phi^{-1} \left[1 + \frac{1}{2}\left(\frac{R}{R_\mathrm{h}}\right)^2\right]^{-1} c^2 dT^2 - \Phi^{-1} dR^2 - R^2 d\Omega^2 \tag{115}$$

4.3.2 Apparent Horizon for Pure Lambda/de Sitter Universe

Again as we see eqs. (67), considering the present-day value of the scale factor scaled to $a_0 = 1$, we get

$$a(t) = e^{H_0 t} \tag{116}$$

The metric of spacetime can be written as

$$ds^2 = c^2dt^2 - e^{2H_0t}\left[dr^2 + r^2d\Omega^2\right] \tag{117}$$

Therefore, since $a = e^{f(t)}$,

$$f(t) = \ln[a(t)] = H_0t \tag{118}$$

Meaning,

$$\dot{f} = H_0 \tag{119}$$

And the radius of the cosmic horizon

$$R_h = c/H_0 \quad \dot{R}_h = 0 \tag{120}$$

From eq. (106), The de Sitter metric stands out from other cosmologies in that the radius R_h is set for all cosmic time t since the density ρ is constant. However, for every other cosmology, we will take a look at below, $w > -1$, which means $\dot{R}_h > 0$. Naturally, this means that, while an observer can select radii R that are always less than R_h in de Sitter, this is not the case when $\dot{R}_h > 0$ because, for any given R, R_h for de Sitter.

$$\Phi^{1/2}cdT \equiv \Phi^{1/2}\left[cdt + \left(\frac{R}{R_\mathrm{h}}\right)\Phi^{-1}dR\right] \tag{121}$$

Calculating the dimensionless integrating factor $\beta(t, R)$

$$\beta(t, R) = \Phi^{-1} \tag{122}$$

Integrating eq. (121), we get

$$T(t, R) = t - \frac{1}{2H_0}\ln\Phi \tag{123}$$

Thereby, the metric becomes

$$ds^2 = \Phi\left[cdt + \left(\frac{R}{ct}\right)\Phi^{-1}dR\right]^2 - \Phi^{-1}dR^2 - R^2d\Omega^2 \tag{124}$$

Naturally, T is equal to t at the origin, but because the gravitationally produced dilation increases with the square of the radius, R, T also includes the extra redshift that is seen as the observer gets further and further away from the source of the dilation. However, keep in mind that given a finite period ds, as $R \to R_h$ for $dR = d\Omega = 0, dT = dt$. Thus, in terms of R and T, the de Sitter metric is

$$ds^2 = \Phi c^2 dT^2 - \Phi^{-1} dR^2 - R^2 d\Omega^2 \tag{125}$$

4.3.3 Apparent Horizon for Lambda CDM Model

Eqs. (51) and (52) show the most accurate representation and the closest values we have to understand the current picture of the universe, as the ΛCDM Model is the most accurate model and set of values we have which predicts the horizon radii of the observable universe. These parameters describe a flat universe whose dynamics are controlled by two enigmatic energy types, most notably the cosmological constant. The argument over whether or not to include the cosmological component in Einstein's theory is now settled; not only should it be included, it also governs the universe. The argument over whether the cosmological constant exists has been settled, but the discussion of its physical ramifications has only begun. The Friedmann equations (8) can be combined for the given values to derive the equation

$$2\frac{\ddot{a}}{a} + \left(\frac{\dot{a}}{a}\right)^2 = \Lambda c^2 \tag{126}$$

This equation can be solved exactly giving the result [38] ($\Lambda = 1.1056 \times 10^{-52} \mathrm{m}^{-2}$)

$$a(t) = A^{1/3} \sinh^{2/3}\left(\frac{t}{t_\Lambda}\right) \tag{127}$$

where

$$A = \Omega_{m,0}/\Omega_{\Lambda,0} \approx 0.43 \quad \text{and} \quad t_\Lambda = \frac{2}{3H_\infty} = \left(\frac{4}{3\Lambda c^2}\right)^{1/2} \approx 3.4 \times 10^{17} \text{ s} \tag{128}$$

where $H_\infty \equiv \lim_{t\to\infty} H(t) \approx 1.96079 \times 10^{-18}\mathrm{s}^{-1}$ is the asymptotic (constant) value of the Hubble constant, which describes a universe that has begun to expand due to cosmological constants. As a result, in Lambda-CDM cosmology,

$$f(t) = \ln[a(t)] = \ln(A) + \frac{2}{3}\ln\left[\sinh\left(t/t_\Lambda\right)\right] \tag{129}$$

Meaning

$$\dot{f} = \frac{2}{3t_\Lambda \tanh\left(t/t_\Lambda\right)} = \frac{H_\infty}{\tanh\left(3tH_\infty/2\right)} \tag{130}$$

thereby, the horizon radius can be derived as it is a trivial condition when $\dot{f}$ has the correct limiting forms (when $t \to \infty$) and (when $t \to 0$).

Therefore,

$$R_\mathrm{h} = \left(\frac{c}{H_\infty}\right)\tanh\left(\frac{3}{2}tH_\infty\right) \quad \dot{R}_\mathrm{h} = \frac{3}{2}c\left[1 - \tanh^2\left(\frac{3}{2}tH_\infty\right)\right] \tag{131}$$

And the metric can also be expressed in a more precise manner as

$$ds^2 = c^2dt^2 - A^{2/3}\sinh^{4/3}\left(t/t_\Lambda\right)\left[dr^2 + r^2d\theta^2 + r^2\sin^2\theta d\phi^2\right] \tag{132}$$

This explains how we might think of the cosmos as an expanding Euclidean sphere, with the expansion being controlled by the expression $a(t)$ found in equation (127). However, take note that the cosmos in this illustration is shown as the sphere's full volume, not simply the surface.

4.4 Comparative study of Horizons in FLRW Models

Graphical representation of horizon radii and its time derivative gives us insight into the behavior and the evolution of the horizon radii in time.

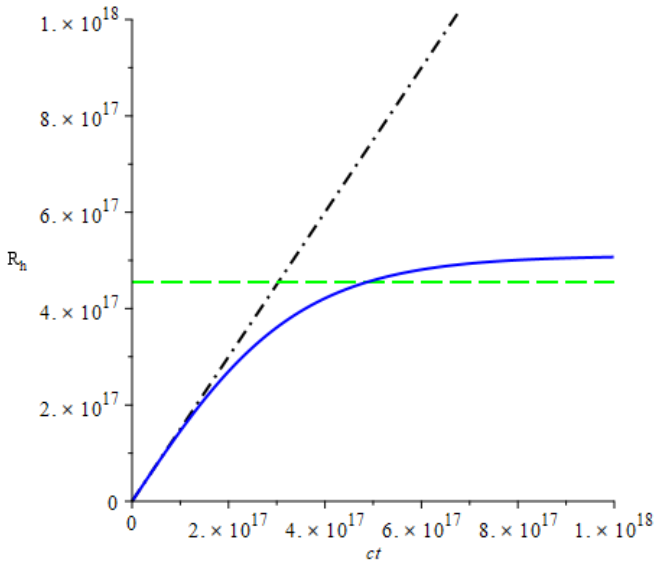

Figure 4.1: Evolution of Horizon Radius R_h in scaled time ct for the given FLRW Models. Einstein-de Sitter model (black dash-dot) (111), Benchmark model (solid blue line) (131), Pure Lambda Universe (green short dash) (120)

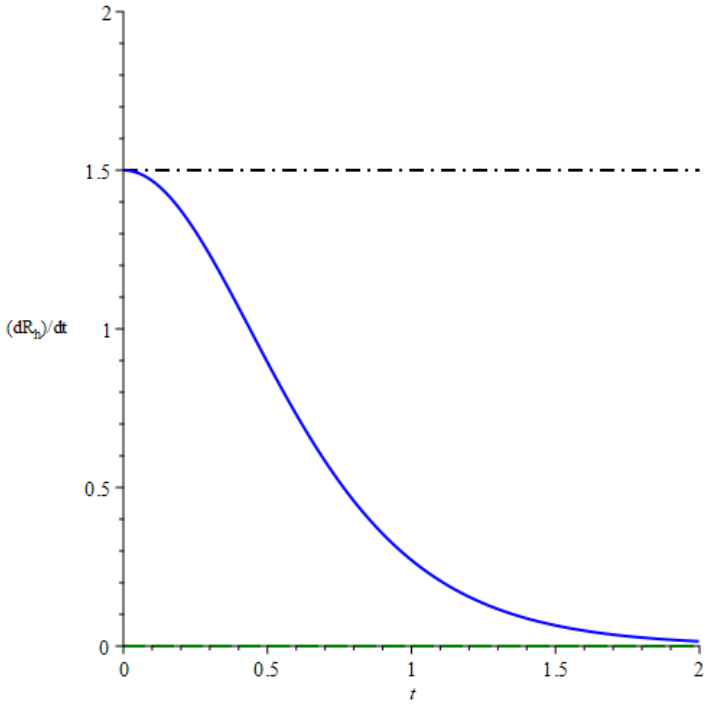

Figure 4.2: An approximation of the evolution of the time derivative of Horizon Radius $\dot{R}_h$ in time t for the given FLRW Models. Einstein-de Sitter model (black dash-dot) (111), Benchmark model (solid blue line) (131), Pure Lambda Universe (green short dash) (120)

.

Chapter 5

Photon paths

Radial photon paths in FLRW (Friedmann–Lemaître–Robertson–Walker) models are trajectories of electromagnetic radiation that can be used to describe the expansion of the universe. Radial photon paths in FLRW models are the result of the expansion of spacetime and the redshift of the light. The relative motion between the observer and the source causes this shift. The expansion of spacetime stretches the wavelength of the radiation, which causes the light to become redder and its intensity to decrease. As the universe expands, the effect of the redshift on the photon paths increases, resulting in the light becoming more and more redshifted. The light from distant galaxies is redshifted to such an extent that it is no longer visible, leading to an 'event horizon' beyond which light cannot be seen.

FLRW models are used to describe the behavior of the universe on the largest scales. These models describe the expansion of space and the redshift of light. The radial photon paths in FLRW models are the paths that light follows as it moves away from its source. As the universe expands, the wavelength of the light becomes stretched, resulting in a redshift. The relative motion between the observer and the source causes this shift. The redshift increases with distance and eventually, the light becomes so redshifted that it can no longer be seen, leading to an 'event horizon'. The event horizon is the point beyond which light cannot be seen. The radial photon paths in FLRW models can be used to describe the expansion of the universe and the relationship between light and space.

A null geodesic is a path that is followed by a massless particle traveling at the speed of light. Since light has no rest mass, it must always travel at the speed of light in vacuum. The trajectory of light rays is influenced by the curvature of spacetime, just like the paths of massive particles. However, since photons have no mass, their paths are not affected by gravity in the same way.

5.1 Null geodesics

Starting from the usual FLRW metric given, if we consider two neighboring points, the spacial increment between the two points can be derived from eq. (4),

$$d\sigma = \left[dr^2/\left(1-kr^2\right) + r^2\left(d\theta^2 + \sin^2\theta d\phi^2\right)\right]^{1/2} \tag{133}$$

and the metric distance between these points will be,

$$dl = a(t)d\sigma \tag{134}$$

We can position ourselves at the origin of spatial coordinates due to the FLRW metric's high degree of symmetry, in which case all photons arriving at this location must have traveled via radial paths in the spatial subspace (by symmetry). A radial distance parameter can be defined.

$$\psi \equiv \int_0^r dx/\left(1-kx^2\right)^{1/2}; \quad d\psi^2 \equiv dr^2/\left(1-kr^2\right) \tag{135}$$

The squared interval for radial paths is

$$ds^2 = c^2dt^2 - a^2d\psi^2 (d\theta = d\phi = 0). \tag{136}$$

The metric (or "ruler") distance between the origin and a simultaneous ($dt = 0$) event is the metric separation

$$l(t) = a\psi = a(t)\int_0^{\psi(t)} d\psi, \tag{137}$$

The metric speed is, therefore,

$$\dot{l} = \dot{a}\psi + a\dot{\psi} = (\dot{a}/a)l + a\dot{\psi} = Hl + a\dot{\psi} \tag{138}$$

But we are considering fixed co-ordinates for dust, meaning $\dot{\psi} = 0$, therefore,

$$\dot{l} = Hl. \tag{139}$$

For radially moving photons, however,

$$\dot{\psi} = \pm c/a. \tag{140}$$

Therefore, the metric speed for photons is

$$\dot{l} = Hl \pm c \tag{141}$$

The main idea and the qualitative response to our initial query are both contained in this equation. First, we observe that photons move at the speed of light where they are, but are dragged by substratum expansion in other locations. The local substratum in their vicinity is expanding much at a rate faster than the speed of light, and even though the early photons are emitted toward us and quite close to us, they are swept out to cosmic distances before they can actually start making headway toward us.

From eq. (22), we can see that

$$\left(\frac{\dot{a}}{a_0}\right)^2 = H_0^2 \left[1 - \Omega_0^{(\mathrm{tot})} + \Omega_{\rho 0}\left(\frac{a}{a_0}\right)^{-(3w+1)} + \Omega_{\Lambda 0}\left(\frac{a}{a_0}\right)^2\right] \tag{142}$$

Which can also be written as

$$\dot{y}^2 = H_0^2 \left[1 - \Omega_0^{(\mathrm{tot})} + \Omega_{\rho 0} y^{-(3w+1)} + \Omega_{\Lambda 0} y^2\right] \tag{143}$$

Where $y = \frac{a}{a_0}$ is the universe expansion function.

$$dy = \pm H_0 f(y) dt; H_0 t = \int_0^y dy/f(y). \tag{144}$$

Where $f(y) = (1 - \Omega_0^{(\text{tot})} + \Omega_{\rho 0} y^{-(3w+1)} + \Omega_{\Lambda 0} y^2)^{\frac{1}{2}}$.

Therefore to understand the behavior of photons in the FLRW models and their evolution in time, it is also important to study the evolution of the models themselves.

5.1.1 Comparitive study of Universe Expansion function for different FLRW Models

For different variations of universes in the FLRW models we look at the universe expansion function

$$\begin{aligned} &H_0 t = \frac{a}{a_0} = \int_0^y dy/f(y) \\ &\text{where, } f(y) = (1 - \Omega_0^{(\text{tot})} + \Omega_{\rho 0} y^{3w+1} + \Omega_{\Lambda 0} y^{-2})^{\frac{1}{2}} \end{aligned} \tag{145}$$

The value considered in this instance is using WMAP data [2]

$$\begin{aligned} H_0 &= 70\,\text{km/s/Mpc} \quad \text{where} \quad 1\text{MPc} \approx 3.26156 \times 10^6\,\text{ly} \\ &\approx 7.1540 \times 10^{-11} (\text{years})^{-1} \end{aligned} \tag{146}$$

$$\text{Hubble Time} \quad t_H = \frac{1}{H_0} \approx 13.9781 \times 10^9 \text{years} \quad \text{Hubble distance} \quad d_H = \frac{c}{H_0} \approx 13.97 \times 10^9\,\text{ly} \tag{147}$$

Universe expansion function $y = \frac{a}{a_0}$ is graphed versus $H_0(t - t_0)$. Which can be scaled to present-day values such that $\frac{a}{a_0} = 1$, and $t = t_0$. Age of the universe t_0 is calculated according to different models considered such that $a_0 = 0$ can be considered as the beginning of the universe or the Big Bang. This can be considered as a study of the evolution of the scale factor a with respect to time, for different models considered. Comparing the evolution of the scale factor in these models, we see that the Einstein-de-Sitter model has a power-law growth of the scale factor, the ΛCDM model has exponential growth, and the Big Crunch model has a decreasing scale factor as the universe collapses. We see

that the Loitering universe model exhibits a phase of decelerated expansion followed by a period of loitering before transitioning to accelerated expansion. On the other hand, the Empty universe model assumes no matter or energy content and results in linear growth of the scale factor over time.

We also see that the Rebounding universe model involves a phase of contraction followed by a bounce and subsequent expansion. The scale factor evolves according to a specific equation with an exponent that determines the behavior during both the contraction and expansion phases. The scale factor grows exponentially over time in the Pure Lambda Universe model, which implies a dominant cosmological constant driving the expansion. These models provide different perspectives on the possible dynamics of the universe and the impact of different components on its evolution. The evolution of the universe expansion function is depicted in the figures given below.

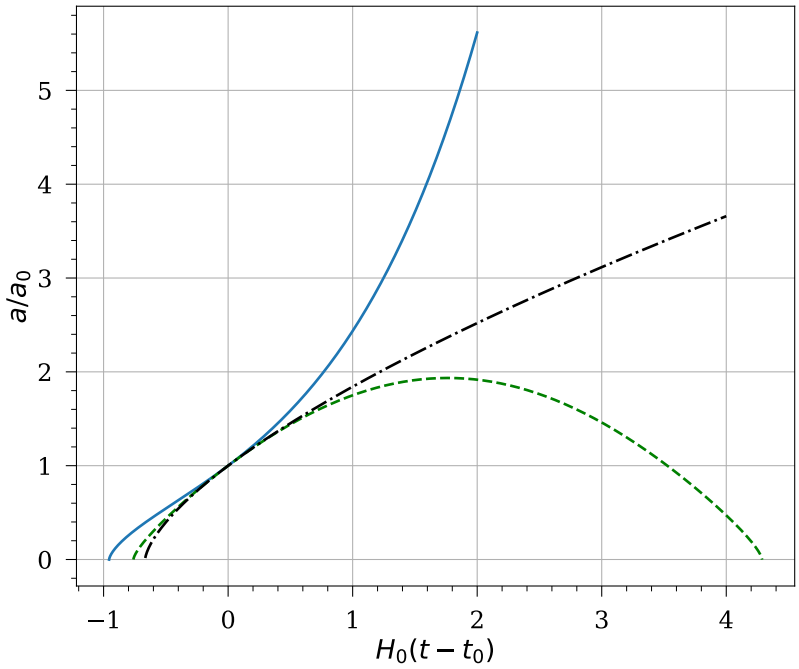

Figure 5.1: Evolution of the Universe expansion function $y = \frac{a}{a_0}$. Age of the universe according to, Einstein-de Sitter model (black dash-dot) $t_0 \approx 0.6667 t_H \equiv 9.3187 \times 10^9$years, Benchmark model (solid blue line) $t_0 \approx 0.9556 t_H \equiv 13.3574 \times 10^9$years, Big Crunch model (green short dash) $t_0 \approx 0.7606 t_H \equiv 10.6317 \times 10^9$years.

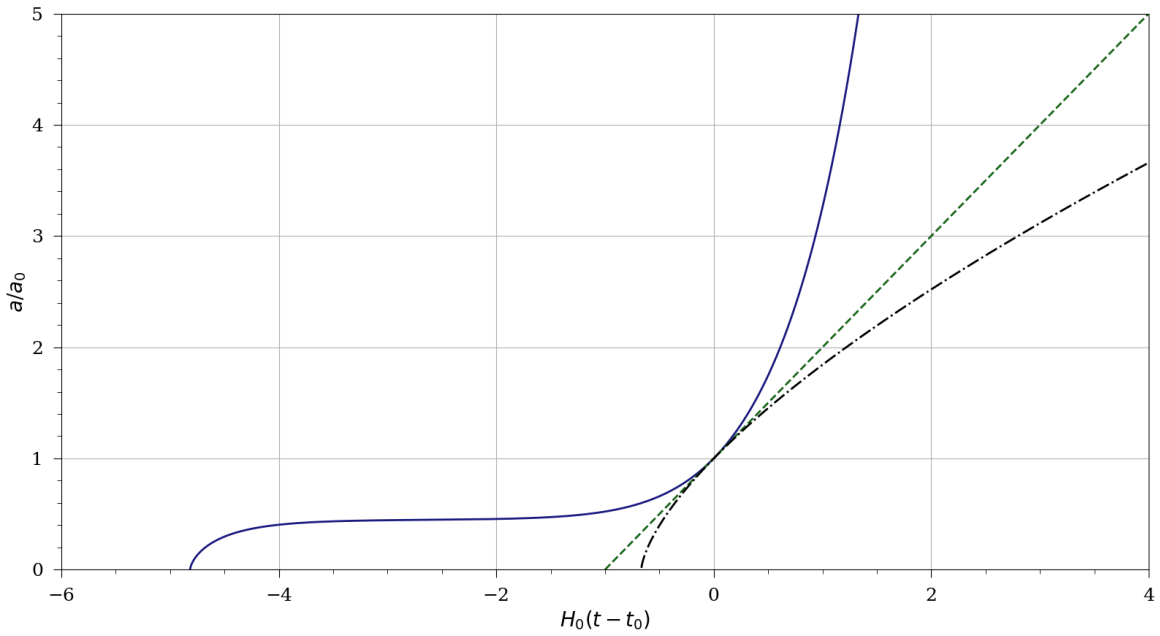

Figure 5.2: Evolution of the Universe expansion function $y = \frac{a}{a_0}$. Age of the universe according to, Einstein-de Sitter model (black dash-dot) $t_0 = 2/3t_H \equiv 9.3187 \times 10^9$years, Loitering Universe (solid blue line) $t_0 \approx 4.8163t_H \equiv 67.3227 \times 10^9$years, Empty Universe (green short dash) $t_0 \approx 1.000t_H \equiv 13.9781 \times 10^9$years

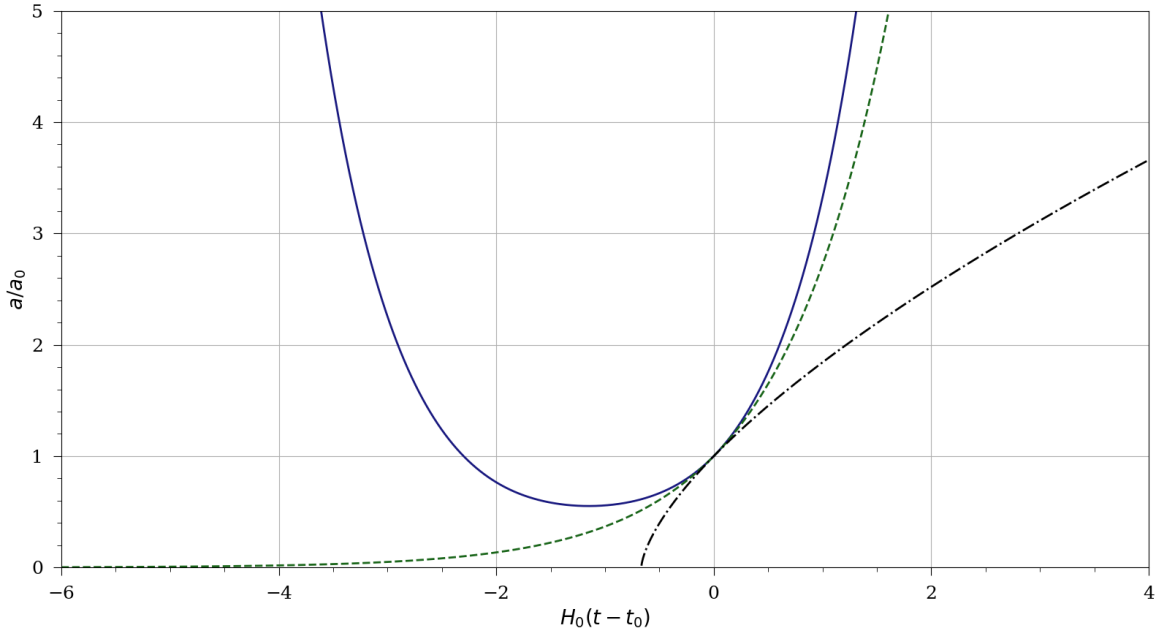

Figure 5.3: Evolution of the Universe expansion function $y = \frac{a}{a_0}$. Einstein-de Sitter model (black dash-dot), Rebouncing Universe (solid blue line), Pure Lmabda Universe (green short dash). (These 2 models do not have a beginning, hence the age cannot be calculated)

5.1.2 Comparitive study of Effective Potential of FLRW Models

The concept of effective potential is a useful tool from classical mechanics to describe the dynamics of one-dimensional motion of the particle in a potential field. It can be used to find turning points and qualitatively describe the allowed space regions for the particle with given mechanical energy. Analogically, this concept can be use to illustrate the dynamics o our models.

From eq, (143), we can see that,

$$\frac{1}{H_0^2}\dot{y}^2 = \left[\frac{dy}{d(H_0 t)}\right]^2 = 1 - U_{ef} \tag{148}$$

where,

$$U_{ef} = \Omega_0^{(\mathrm{tot})} - \Omega_{\rho 0} y^{-(3w+1)} - \Omega_{\Lambda 0} y^2. \tag{149}$$

The plots of the effective potentials for our models have been graphed in Figs. 5.4–5.6, the turning points (in which the expansion turns into the collapse or vice versa) are given by the condition $U_{ef} = 1$ following from eq. (148) and $\dot{y} = 0$. While the Benchmark, Loitering and Rebouncing models have similar shapes where it represents an increase then a decrease with respect to the scale factor, models like the Big Crunch has an ever increasing potential and empty universe as zero effective potential.

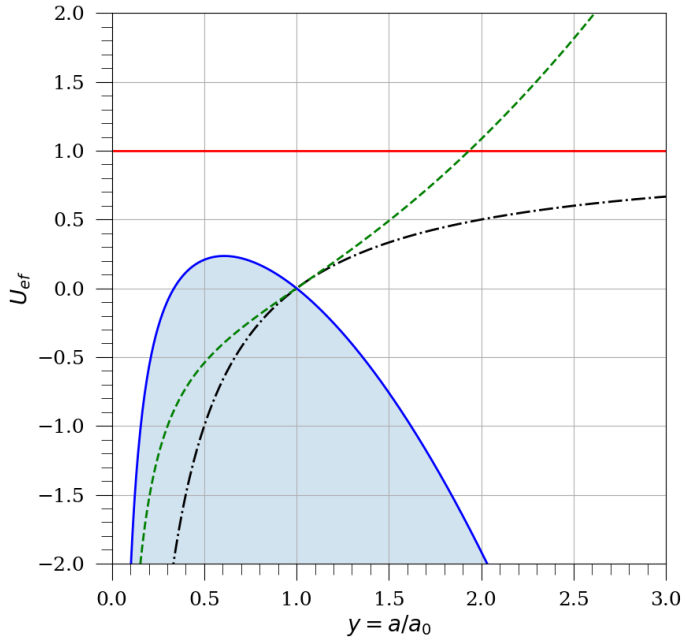

Figure 5.4: Effective Potential U_{ef} versus y for the given FLRW Models. Einstein-de Sitter model (black dash-dot), Benchmark model (solid blue line), Big Crunch model (green short dash)

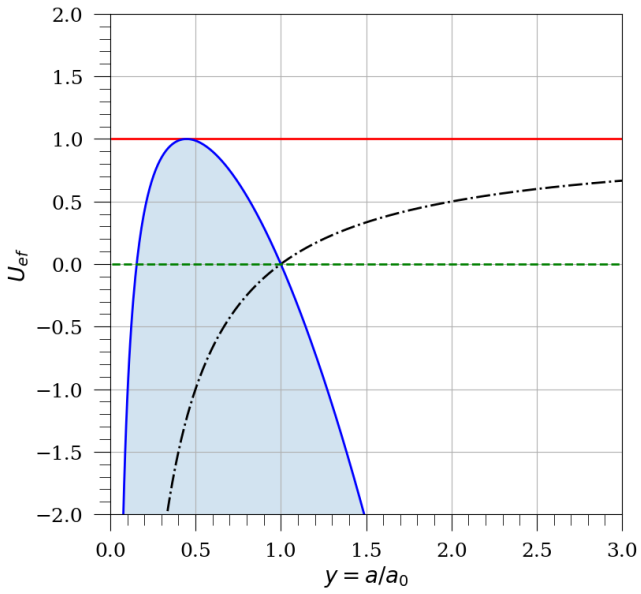

Figure 5.5: Effective Potential U_{ef} versus y for the given FLRW Models. Einstein-de Sitter model (black dash-dot), Loitering Universe (solid blue line), Empty Universe (green short dash).

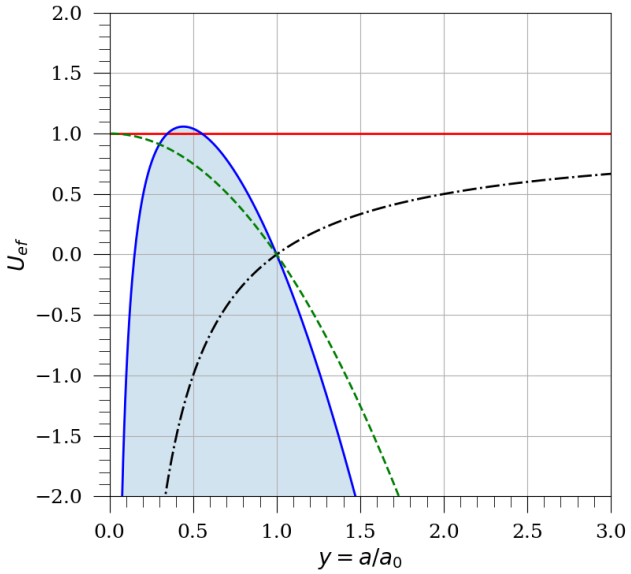

Figure 5.6: Effective Potential U_{ef} versus y for the given FLRW Models. Einstein-de Sitter model (black dash-dot), Rebouncing Universe (solid blue line), Pure Lambda Universe (green short dash).

5.1.3 Comoving and Proper Distances

Proper distance, also known as physical distance, is a distance measure that cosmologists use to describe distances between objects in standard cosmology. The location of a distant object at a particular point in cosmological time, which can change over time due to the universe's expansion, roughly corresponds to the proper distance. While so called comoving distance is given by the comoving coordinates (r or ϕ as defined in eqs. 4, 5)) and remains constant in time, the proper distance takes the universe's expansion into account.

In cosmology, proper distance is a measure of the physical distance between two points in the universe, taking into account the expansion of space. It is a fundamental concept used to describe the large-scale structure of the universe. Proper distance differs from other distance measures, such as comoving distance or luminosity distance, which are also commonly used in cosmology.

The following equation can be used to determine the appropriate separation between two

places in the expanding universe:

$$d\left(t_0\right) = c\int_{t_e}^{t_0} \frac{dt}{a(t)} \tag{150}$$

$$d\left(t_e\right) = d\left(t_0\right)\frac{a}{a_0} \tag{151}$$

where $d\left(t_0\right)$ can be defined as the proper distance as noticed by the observer and $d\left(t_e\right)$ can be defined as the proper distance during the time of emission from the light source.

The scale factor depicts the universe's relative expansion across time as compared to the present. To calculate the proper distance, one needs to integrate the expression over the cosmic time interval between the two points. This integration accounts for the expansion of the universe, as the scale factor changes with time. The result is multiplied by the speed of light to obtain a distance measurement. From the resulting graphs, we can observe that similar models have similar evolution of proper distances with respect to time.

The proper distance in the Einstein-de Sitter model increases linearly with time in the near past or future, as the universe expands. In the ΛCDM (Benchmark) model, proper distance will increase at an accelerating rate due to exponential expansion in the future, whereas in the Big Crunch model, proper distance will decrease as the universe contracts toward a collapse. In the Loitering universe model, the proper distance increases during the loitering phase at a slower rate compared to standard expanding models, and then accelerates during the transition to accelerated expansion.

In the Loitering model, the evolution of proper distance with respect to time is characterized by a prolonged period of relatively slow expansion during the loitering phase. The proper distance between objects increases during this phase but at a slower rate compared to the standard expanding models. Eventually, as the universe transitions to accelerated expansion, the proper distance starts to increase at a faster rate. However in the Empty universe model, the proper distance increases linearly with time at a constant

rate due to the absence of matter and energy contributions and is purely geometrical.

In the Rebouncing model, the evolution of proper distance with respect to time is characterized by a contraction phase where the proper distance between objects decreases. After the bounce, when the universe transitions to the expanding phase, the proper distance starts to increase again. The rate of increase in the proper distance during the expanding phase depends on the specific dynamics and assumptions of the model. The cosmological constant governs the expansion of the universe in the Pure Lambda model, which causes the scale factor to rise exponentially as time passes. As a result, the proper distance between objects increases at an accelerating rate. The physical distance between two objects expands exponentially with time due to the constant and dominant effect of dark energy. An important feature to notice in the proper distance graphs potted below is that the integration and negative time depicts a light ray coming from the past into the the present. That is, we are viewing a distant light ray to measure the proper distance.

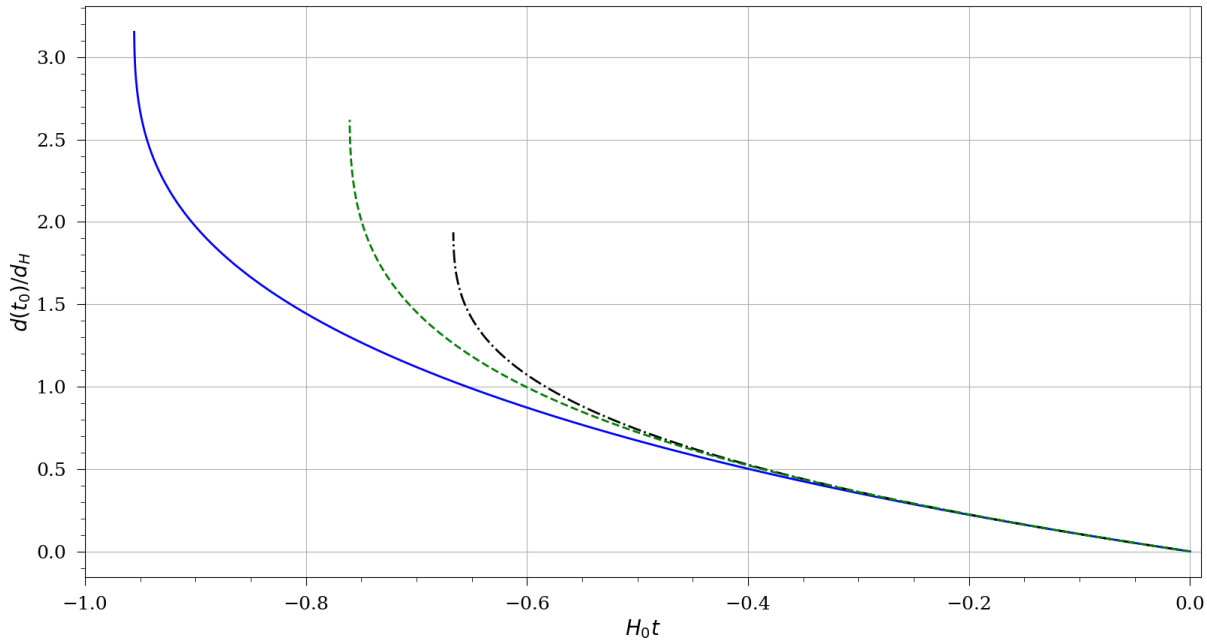

Figure 5.7: Proper distance during time of observation (scaled) $d(t_0)/d_H$ versus Time (scaled) $H_0 t$ for the given FLRW Models. Einstein-de Sitter model (black dash-dot), Benchmark model (solid blue line), Big Crunch model (green short dash)

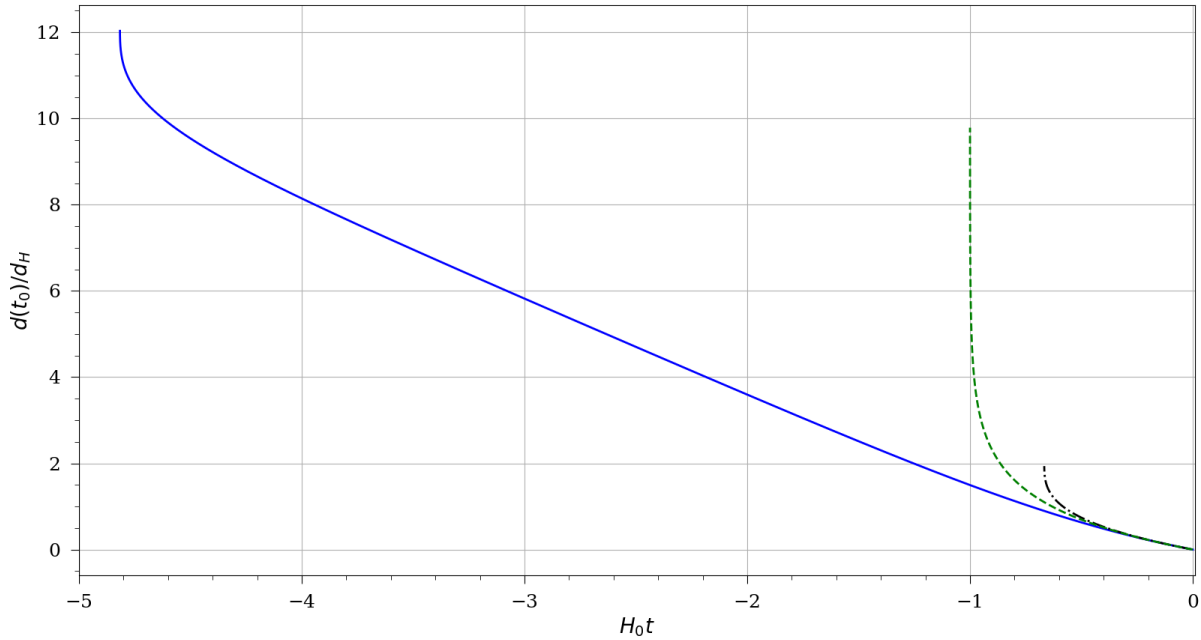

Figure 5.8: Proper distance during time of observation (scaled) $d(t_0)/d_H$ versus Time (scaled) H_0t for the given FLRW Models. Einstein-de Sitter model (black dash-dot), Loitering Universe (solid blue line), Empty Universe (green short dash).

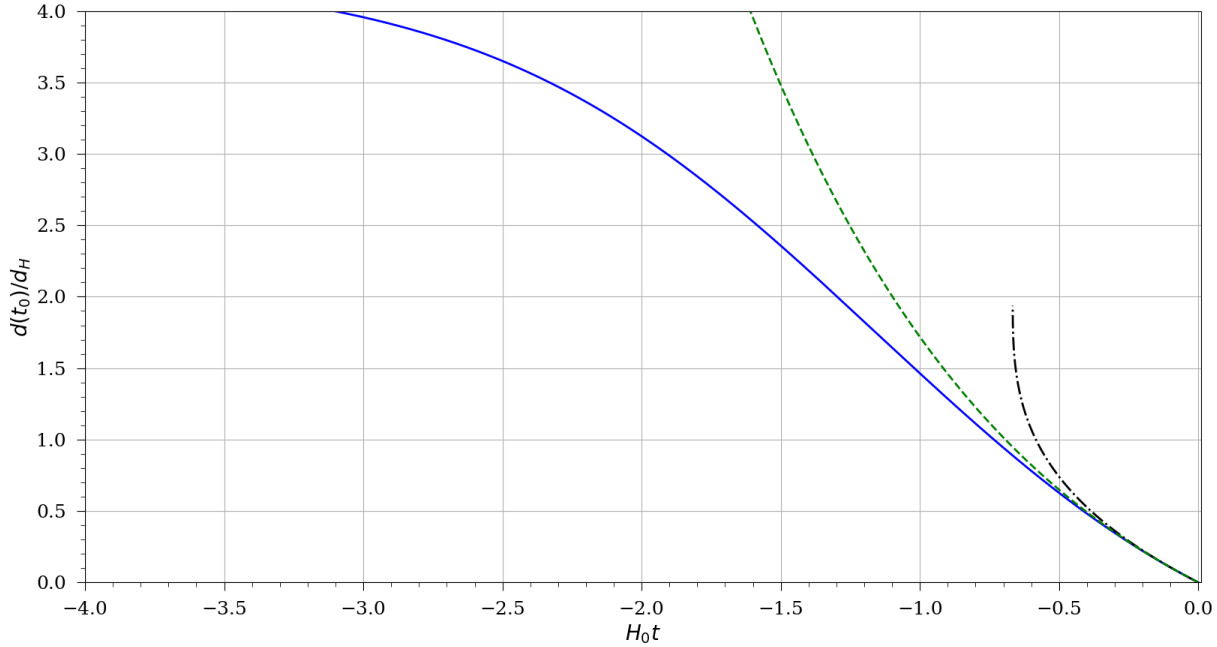

Figure 5.9: Proper distance during time of observation (scaled) $d(t_0)/d_H$ versus Time (scaled) H_0t for the given FLRW Models. Einstein-de Sitter model (black dash-dot), Rebouncing Universe (solid blue line), Pure Lambda Universe (green short dash).

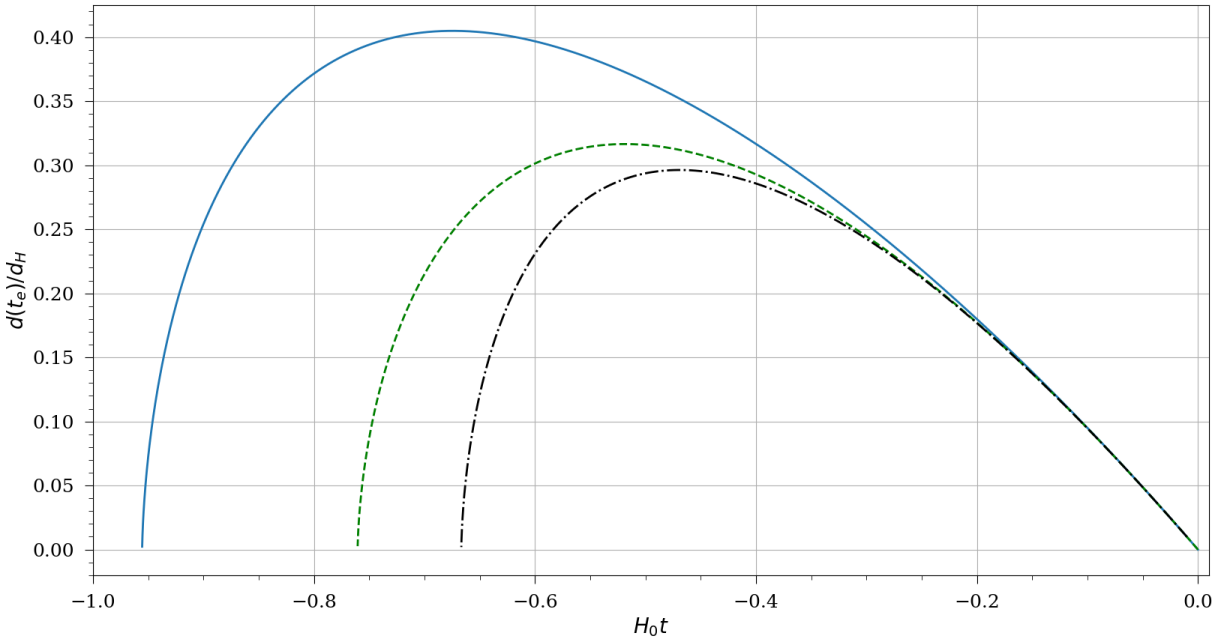

Figure 5.10: Proper distance during time of emission (scaled) $d(t_e)/d_H$ versus Time (scaled) H_0t for the given FLRW Models. Einstein-de Sitter model (black dash-dot), Benchmark model (solid blue line), Big Crunch model (green short dash)

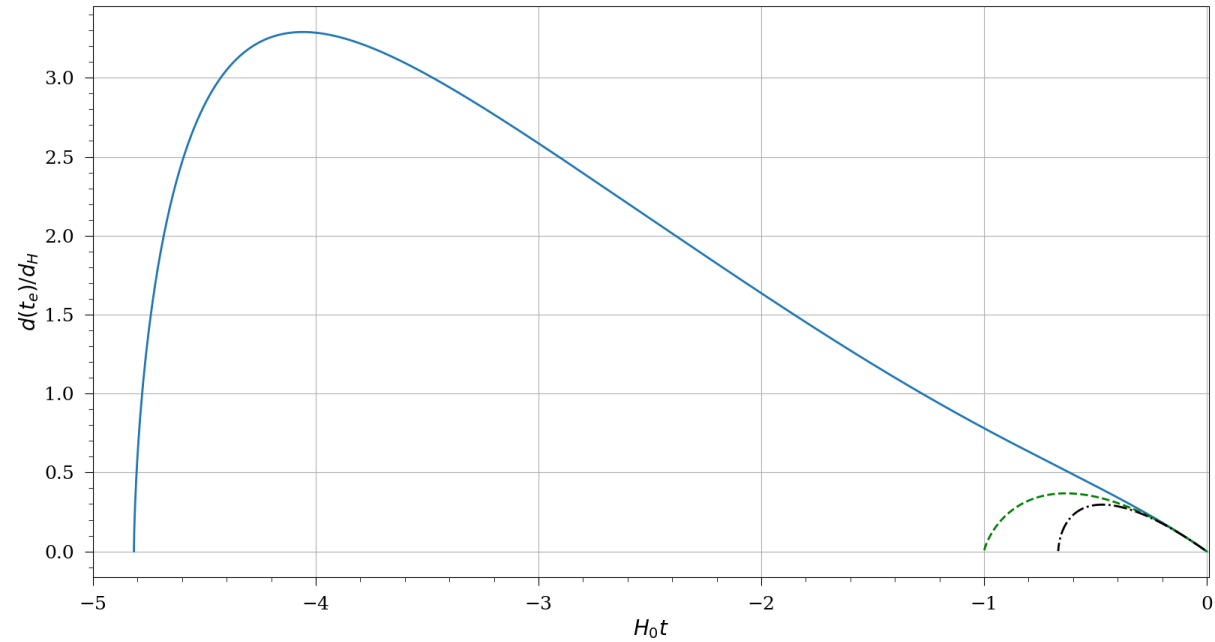

Figure 5.11: Proper distance during time of emission (scaled) $d(t_e)/d_H$ versus Time (scaled) H_0t for the given FLRW Models. Einstein-de Sitter model (black dash-dot), Loitering Universe (solid blue line), Empty Universe (green short dash).

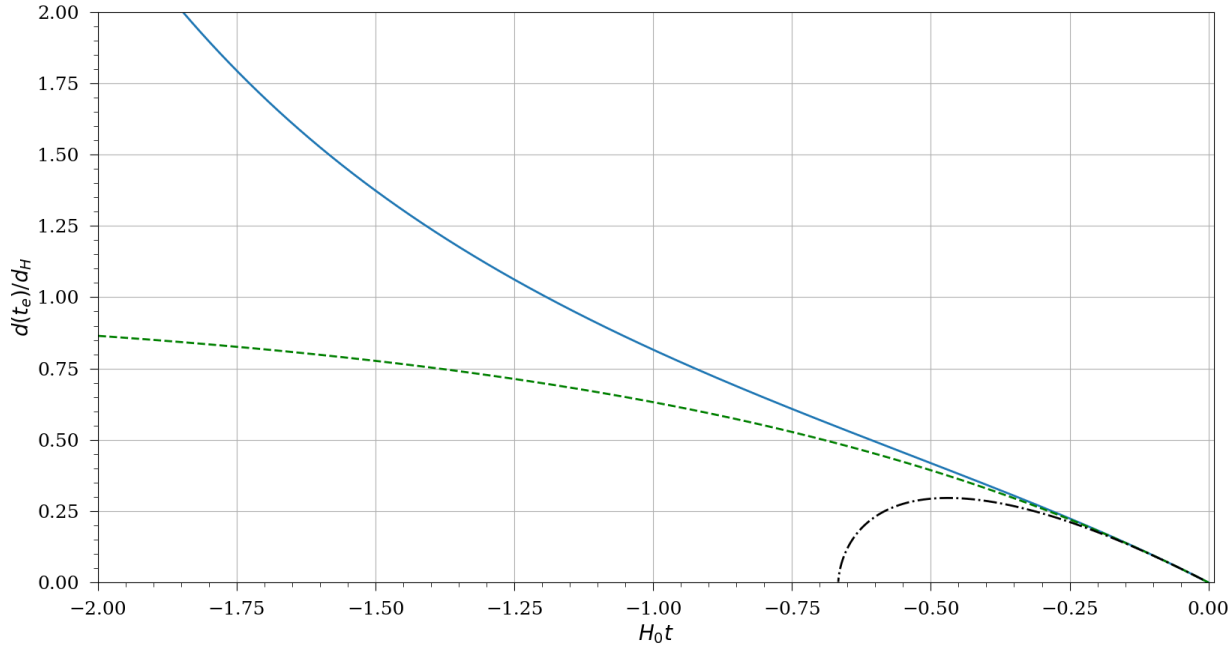

Figure 5.12: Proper distance during time of emission (scaled) $d(t_e)/d_H$ versus Time (scaled) H_0t for the given FLRW Models. Einstein-de Sitter model (black dash-dot), Rebouncing Universe (solid blue line), Pure Lambda Universe (green short dash).

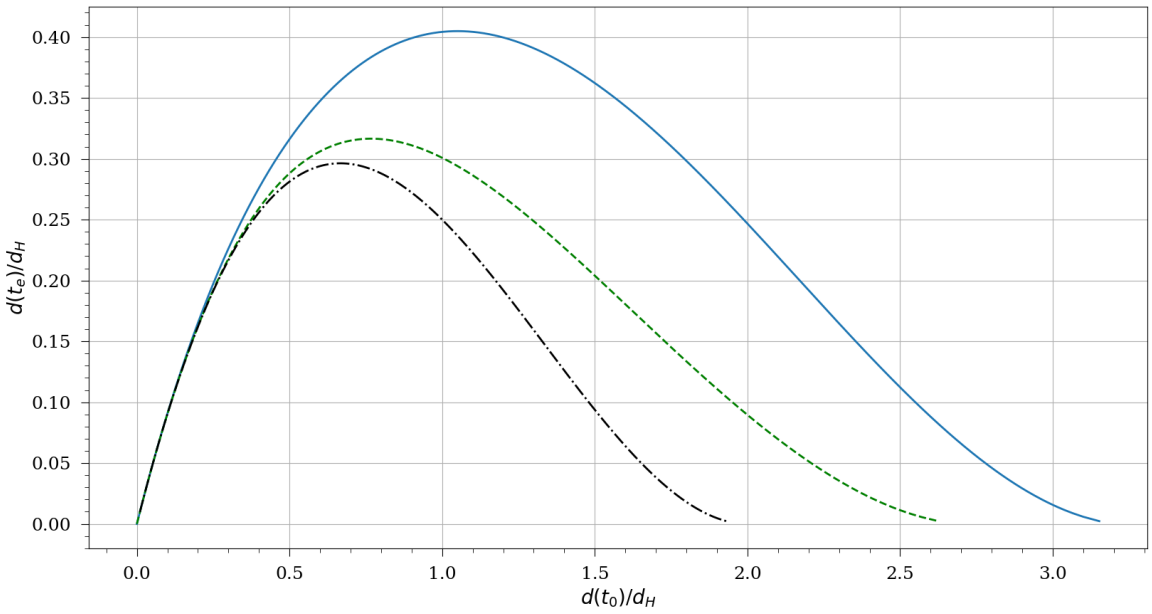

Figure 5.13: Proper distance during time of emission (scaled) $d(t_e)/d_H$ versus Proper distance during time of observation (scaled) $d(t_O)/d_H$ for the given FLRW Models. Einstein-de Sitter model (black dash-dot), Benchmark model (solid blue line), Big Crunch model (green short dash)

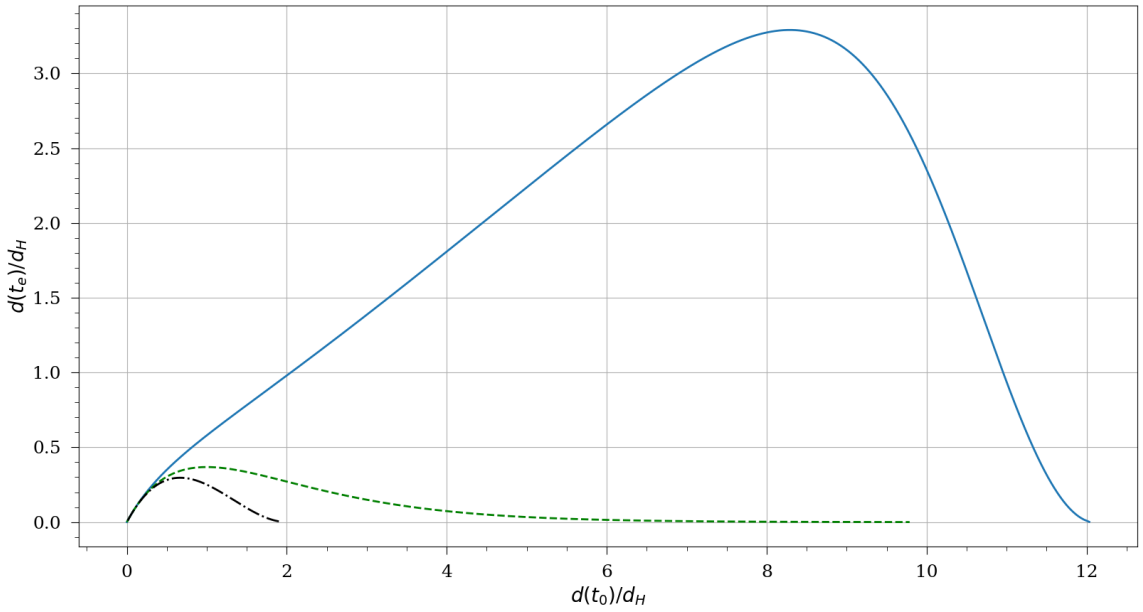

Figure 5.14: Proper distance during time of emission (scaled) $d(t_e)/d_H$ versus Proper distance during time of observation (scaled) $d(t_O)/d_H$ for the given FLRW Models. Einstein-de Sitter model (black dash-dot), Loitering Universe (solid blue line), Empty Universe (green short dash).

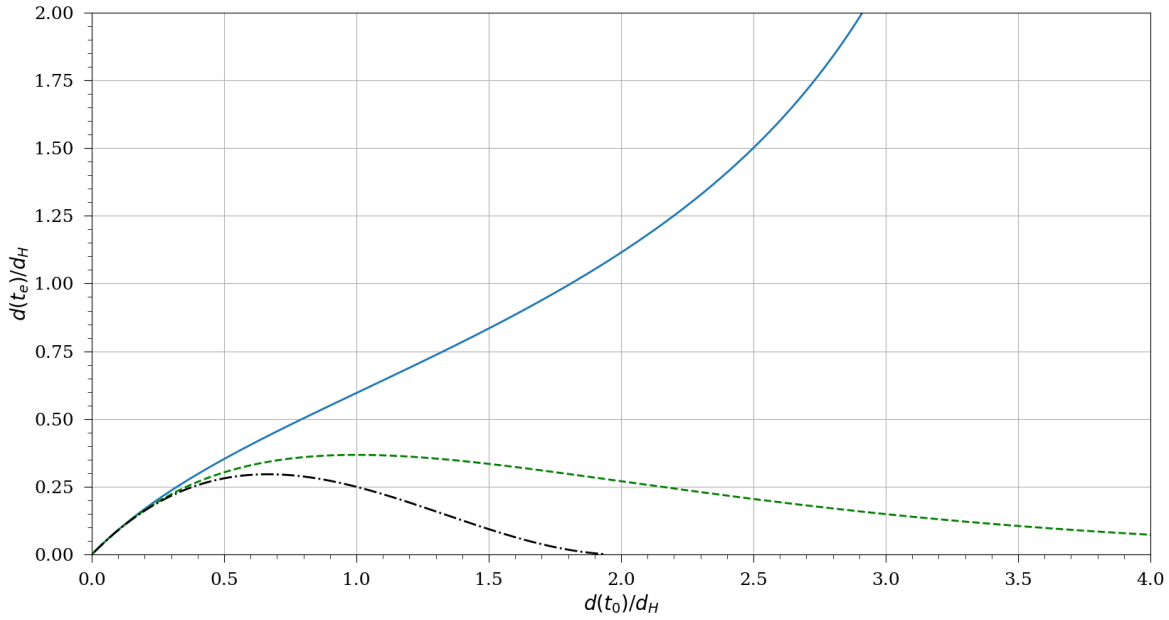

Figure 5.15: Proper distance during time of emission (scaled) $d(t_e)/d_H$ versus Proper distance during time of observation (scaled) $d(t_O)/d_H$ for the given FLRW Models. Einstein-de Sitter model (black dash-dot), Rebouncing Universe (solid blue line), Pure Lambda Universe (green short dash).

It's important to note that the proper distance is not directly observable, as we cannot measure distances on cosmological scales with a ruler. Instead, astronomers and cosmologists use various techniques and observations, such as redshifts and the cosmic microwave background, to infer distances and calculate cosmological parameters. In practice, the proper distance is often measured in terms of redshift. Proper distance equation can be rewritten in terms of redshift:

$$d = c \int \frac{(1+z)}{H(z)} dz \tag{152}$$

where

$$H(z) \approx H_0 \sqrt{\Omega_{\rho 0}(z+1)^{3w+1} + \Omega_k (z+1)^2 + \Omega_{\Lambda 0}}, \quad \left(\Omega_k = \frac{kc^2}{a^2 H^2}\right)$$

is the Hubble parameter as a function of redshift, which describes the rate of expansion of the universe at a given redshift. Overall, proper distances provide a way to understand the physical separation between objects in the universe, accounting for the expansion of space. They are essential for studying the large-scale structure and evolution of the cosmos.

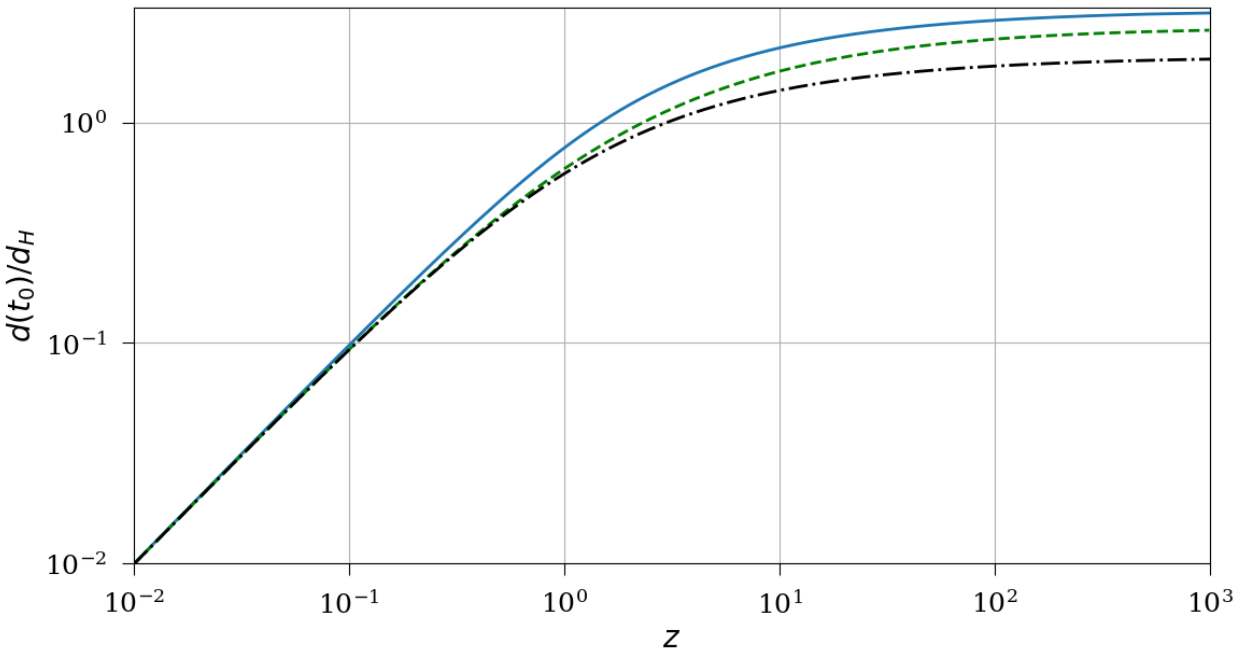

Figure 5.16: Proper distance during time of observation (scaled) $d(t_O)/d_H$ versus redshift z for the given FLRW Models. Einstein-de Sitter model (black dash-dot), Benchmark model (solid blue line), Big Crunch model (green short dash)

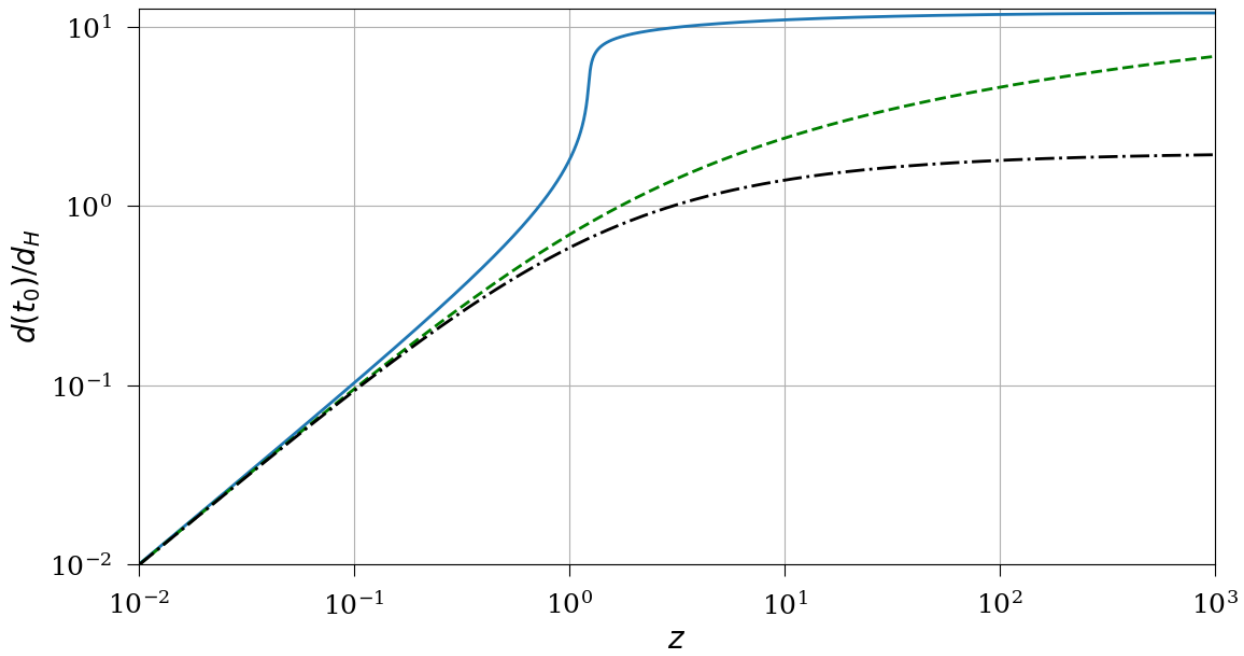

Figure 5.17: Proper distance during time of observation (scaled) $d(t_O)/d_H$ versus redshift z for the given FLRW Models. Einstein-de Sitter model (black dash-dot), Loitering Universe (solid blue line), Empty Universe (green short dash).

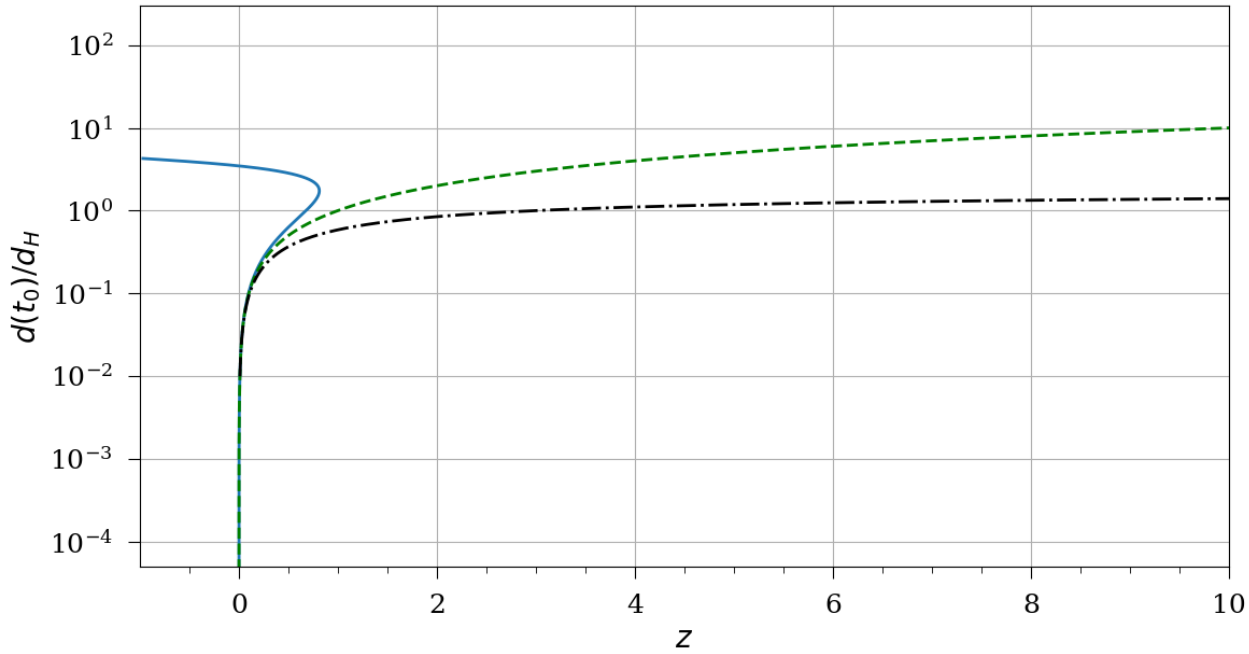

Figure 5.18: Proper distance during time of observation (scaled) $d(t_O)/d_H$ versus redshift z for the given FLRW Models. Einstein-de Sitter model (black dash-dot), Rebouncing Universe (solid blue line), Pure Lambda Universe (green short dash).

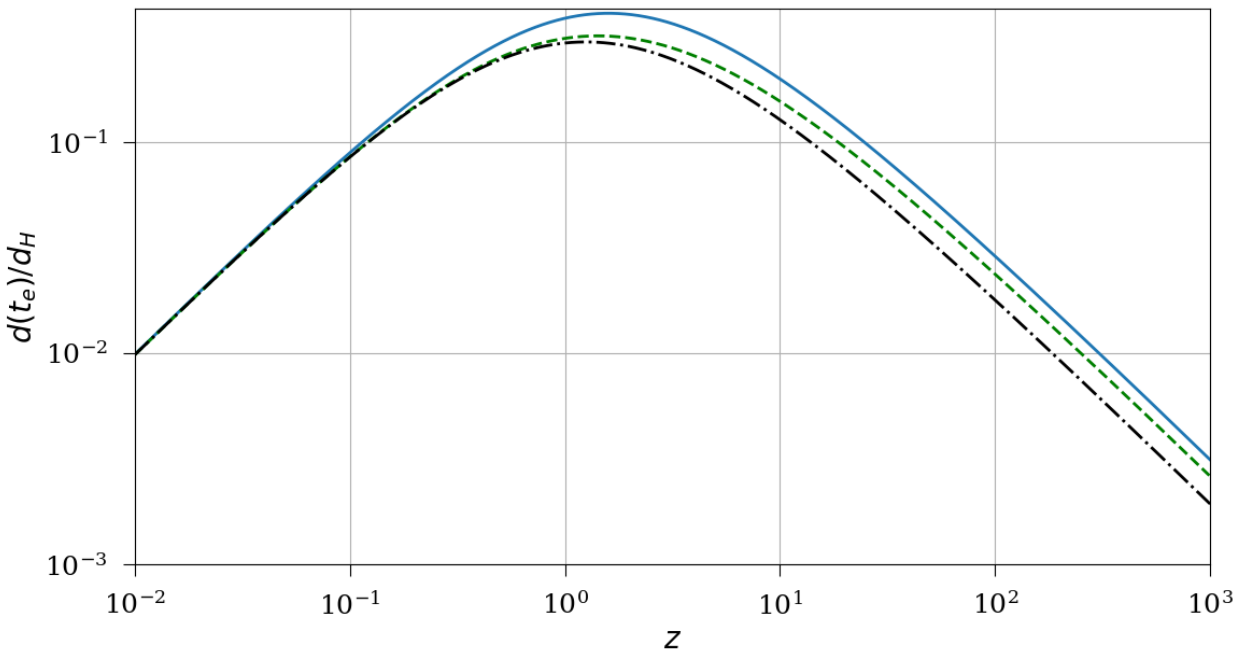

Figure 5.19: Proper distance during time of emission (scaled) $d(t_e)/d_H$ versus Redshift z for the given FLRW Models. Einstein-de Sitter model (black dash-dot), Benchmark model (solid blue line), Big Crunch model (green short dash)

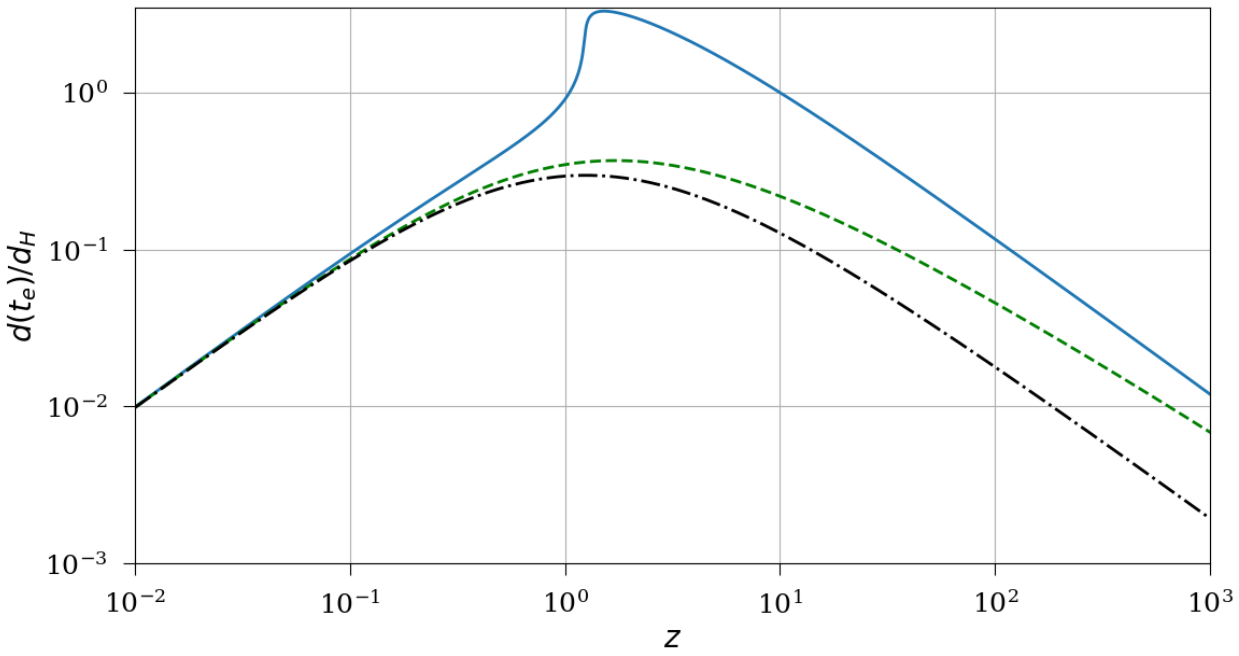

Figure 5.20: Proper distance during time of emission (scaled) $d(t_e)/d_H$ versus Redshift z for the given FLRW Models. Einstein-de Sitter model (black dash-dot), Loitering Universe (solid blue line), Empty Universe (green short dash).

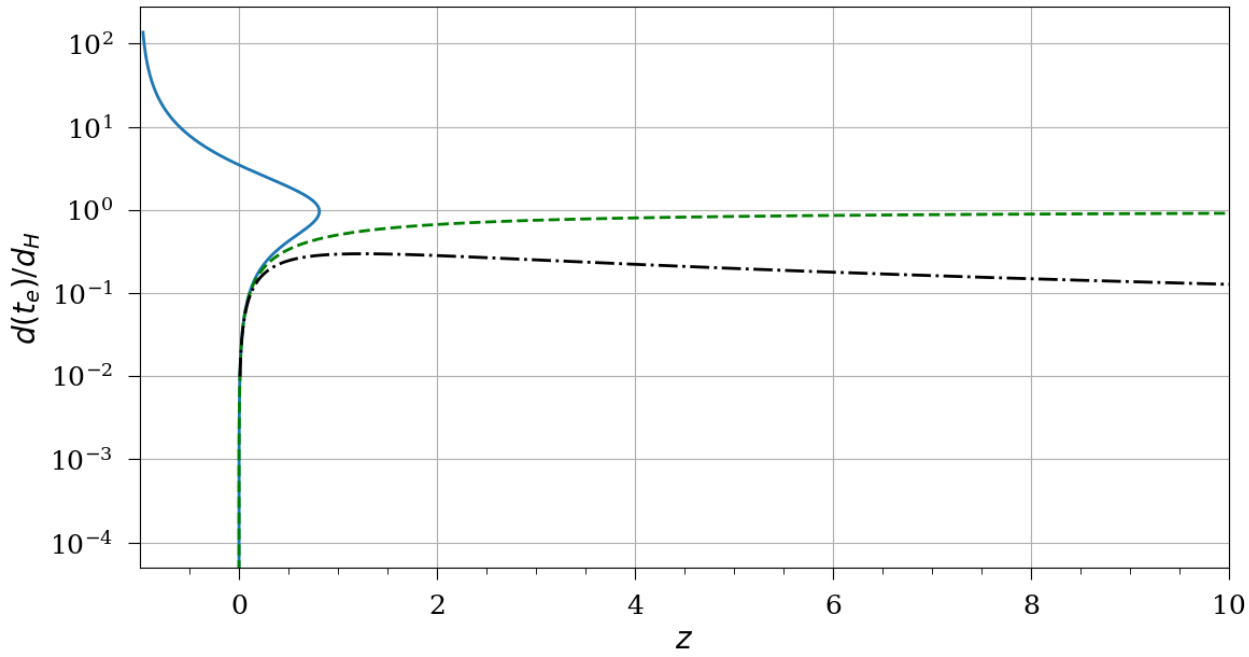

Figure 5.21: Proper distance during time of emission (scaled) $d(t_e)/d_H$ versus Redshift z for the given FLRW Models. Einstein-de Sitter model (black dash-dot), Rebouncing Universe (solid blue line), Pure Lambda Universe (green short dash).

In the Einstein-de-Sitter model, Benchmark model and Big Crunch model the proper distance increases linearly with redshift according to the Hubble law. In the Loitering universe model, the relationship between proper distance and redshift is influenced by the deceleration and loitering phase before transitioning to accelerated expansion. The precise evolution of proper distance with respect to redshift would depend on the specific dynamics and assumptions of the model, while in the Empty universe model, the proper distance increases linearly with redshift according to the standard cosmological relation (Hubble law) due to the absence of matter or energy contributions. For the Rebouncing universe model, the relationship between proper distance and redshift can be more complex, with negative redshift values during the contraction phase and positive redshift values during the expanding phase. In the Pure Lambda Universe model, the proper distance increases linearly with redshift according to the standard cosmological relation, reflecting the exponential expansion driven by the cosmological constant.

5.2 Plotting photon paths for different FLRW Models

We take advantage of the fact that photons have a null interval in order to trace the photon trajectory backward in time beginning at time t_0. As a result, we can calculate the radial distance parameter as a function of the expansion parameter for each point along the reverse trajectory. From eq. (5, 141),

$$\begin{aligned} \dot{\psi} &= -c/a \\ d\psi &= -cda/a\dot{a} = -\left(c/a_0\right) dy/y\dot{y} = -\left(c/a_0 H_0\right) dy/yf(y) \\ \psi(y) &= -\left(c/a_0 H_0\right) \int_1^y dy/yf(y) = +\left(c/a_0 H_0\right) \phi(y) \end{aligned} \tag{153}$$

The figures below show the universal photon curve or photon paths ψ. On this map, galaxies move along the vertical lines of constant $\phi = a_0 H_0 \psi/c$. The curve is a photon trajectory moving from left to right. The curve is bounded in the ϕ domain and can be moved sideways to intercept the time axis at any desired point.

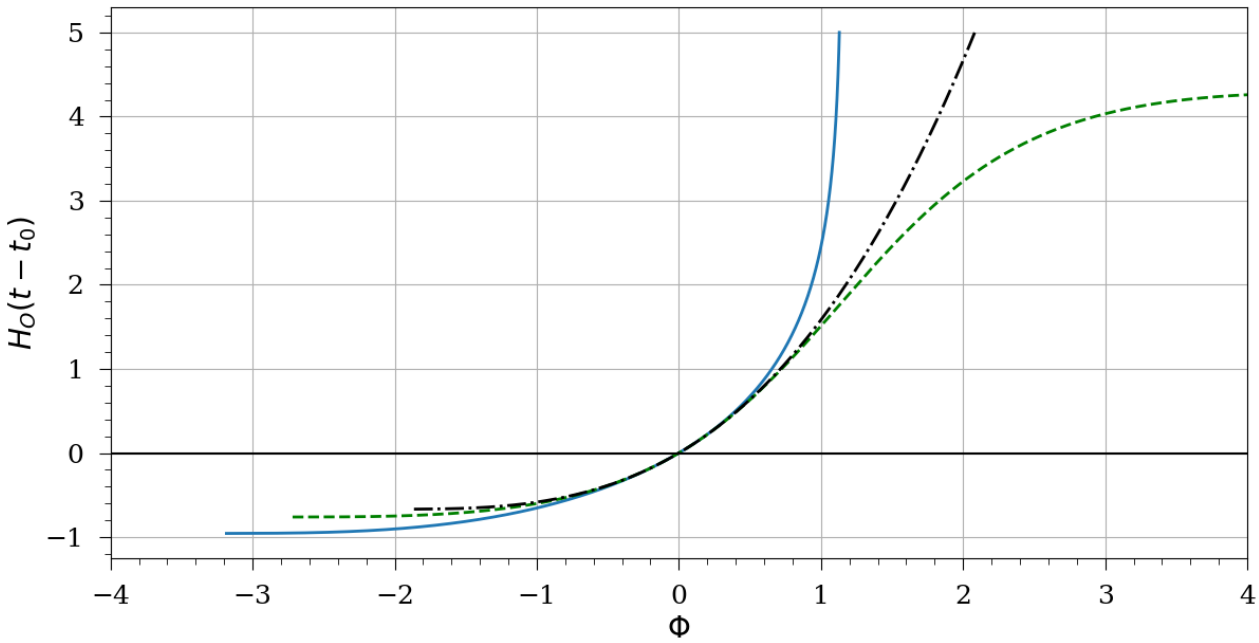

Figure 5.22: Time (scaled) $H_0(t-t_0)$ versus- ϕ for the given FLRW Models. Einstein-de Sitter model (black dash-dot), Benchmark model (solid blue line), Big Crunch model (green short dash).

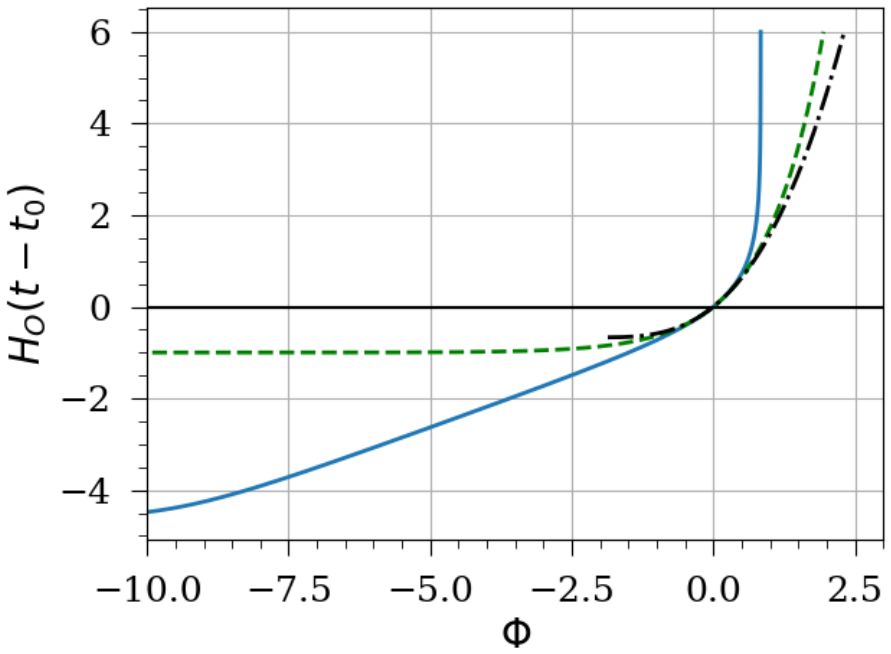

Figure 5.23: Time (scaled) $H_0(t-t_0)$ versus- ϕ for the given FLRW Models. Einstein-de Sitter model (black dash-dot), Loitering Universe (solid blue line), Empty Universe (green short dash).

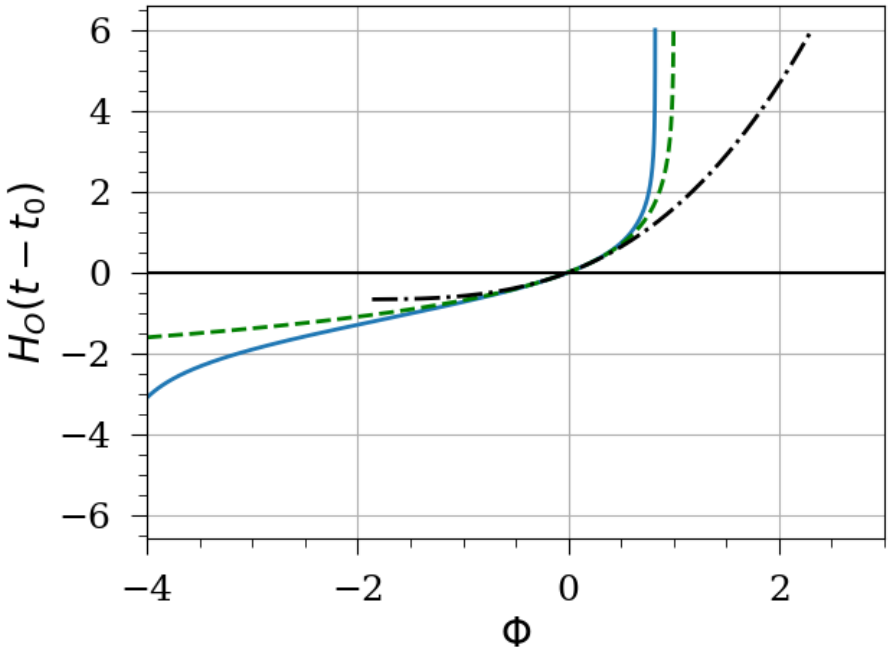

Figure 5.24: Time (scaled) $H_0(t-t_0)$ versus- ϕ for the given FLRW Models. Einstein-de Sitter model (black dash-dot), Rebouncing Universe (solid blue line), Pure Lambda Universe (green short dash).

Chapter 6

Epilogue

In conclusion, this thesis delves into an in-depth exploration of lookback times, horizons, and photon paths within the framework of Friedmann–Lemaıtre–Robertson–Walker cosmological models. By examining various aspects of these models, including their mathematical formulations, physical interpretations, and observational implications, we have gained valuable insights into the nature of the universe and its evolution.

Throughout this study, we have analyzed the concept of lookback time, which allows us to observe distant astronomical objects as they were in the past. We have examined how the expansion of the universe affects the observed properties of these objects, leading to a time delay in the detection of their light. By utilizing the FLRW metric and integrating the equations of motion, we have derived mathematical expressions for calculating lookback times in different cosmological scenarios. We can observe from the lookback time graphs that it greatly depends on the content of the matter, leading to unique graphs for models like the loitering universe and the rebouncing model, although most other models have a structure that is almost generic. It's also important to note that even the graphs for the empty universe and the Pure Lambda universe are remarkably uniform. The graph in the Rebouncing model shows both an increase and a drop in redshift, indicating a blue shift when the cosmos begins to contract back down with a negative scale factor at some future time. However, the generic models share certain similarities in shape. The lookback time will be shorter for low redshifts, corresponding to a more recent period in the history of the universe. The lookback time will increasingly lengthen as redshift rises,

showing that the visible objects are getting older. The graph's slope can first get steeper. The lookback period will grow dramatically at higher redshifts, nearing the early cosmos (big z values), indicating light emitted from far-off and far earlier cosmic epochs.

Additionally, we have investigated the concept of horizons, which define the boundaries beyond which certain events or information cannot be observed. By considering the cosmological redshift, we have explored the relationship between the observed wavelength of light from distant sources and the expansion of space. This has allowed us to understand how the horizon distance evolves over time and how it influences our ability to gather information about the universe. In the ΛCDM model, the apparent horizon radius is not a fixed quantity but evolves with time. It depends on the expansion history of the universe, which is determined by the matter and dark energy content. As the universe expands, the scale factor increases, causing the apparent horizon radius to grow over time. The rate of growth depends on the specific values of the matter density, dark energy density, and the equation of state for dark energy. The apparent horizon radius in the ΛCDM model represents the size of the causally connected region of the universe. The de Sitter Universe is a special case where the apparent horizon radius remains constant over time. This is because the de Sitter Universe is dominated by a cosmological constant (dark energy), which leads to the exponential expansion of the universe. In this scenario, the Hubble parameter remains constant, and consequently, the apparent horizon radius does not change with time. The apparent horizon radius in the de Sitter Universe represents the maximum distance from which a signal can reach an observer at a given time. In the Einstein-de Sitter Universe, the apparent horizon radius also evolves with time. However, unlike the ΛCDM model, the evolution is simpler as it is a matter-dominated universe without dark energy. The apparent horizon radius increases with time, following a different rate of growth compared to the ΛCDM model. In the Einstein-de Sitter Universe, the Hubble parameter and the matter density determine the expansion history and, consequently, the evolution of the apparent horizon radius. The apparent horizon radius in this model represents the size of the causally connected region of the universe. Overall, the apparent horizon radius in these cosmological models captures important aspects of

the universe's expansion and the causal structure. While the de Sitter Universe has a constant apparent horizon radius due to the dominance of dark energy, both the ΛCDM model and the Einstein-de Sitter Universe exhibit time-dependent apparent horizon radii, reflecting the dynamic nature of the universe in the presence of matter and energy components.

Furthermore, we have examined the trajectories of photons in FLRW cosmological models, analyzing their paths through expanding space. By integrating the null geodesic equations, we have determined the equations of motion for photons and explored how their trajectories are influenced by the curvature of spacetime and the expansion of the universe. This analysis has provided us with a deeper understanding of how light propagates through cosmological models and how it is affected by various factors such as the expansion of the universe and the matter content of the universe. Mapping out photon paths in the expanding universe shows the curvature of light in the scale of Hubble time. This also precludes to redshift which will be caused and it is interesting to see how much redshift is happening as we change the curvature and the configuration of the universe. And for that, intricate studies about the evolution of the scale factor and proper distances were required.

When we compare the scale factor evolution in different theories, we find that the ΛCDM model exhibits exponential growth, the Big Crunch model exhibits a decreasing scale factor as the universe contracts. The Einstein-de-Sitter model exhibits a power-law growth of the scale factor. The Loitering universe model, as we can see, depicts a phase of decelerated expansion followed by a time of loitering before changing to accelerated expansion. The scale factor grows linearly over time in the Empty Universe Model, in contrast, which makes no assumptions about the presence of matter or energy. We can also see that the Rebounding universe model includes three phases: contraction, bounce, and expansion.

Overall, this study has shed light on the intricate interplay between lookback times, horizons, and photon paths in FLRW cosmological models. We see subtle differences in the curvature of photons according to the expansion of space-time and matter content. There

are also differences in the age of the universe when studied for different models. We can observe peculiar properties for the likes of the Big Crunch and Loitering Universe on par with their unique properties. The same goes for Pure Lambda Universe and Empty Universe models for which the light seems to take very little time to reach the observer in the present. Whereas most of the other models which are more realistic, and closer to observable values have more generic shapes aligning with the current observations of a flat universe with both matter(baryonic and dark) as well as dark energy, although varying those configurations gave us interesting results in terms of photon curvature and its course in the dynamic continuum of space-time. The knowledge and insights gained from this research can contribute to our understanding of the universe's structure, evolution, and the nature of light propagation within it. As we continue to explore and unravel the mysteries of our cosmos, the findings presented in this thesis will serve as a foundation for future investigations and contribute to advancements in cosmology and astrophysics.

Bibliography

[1] M. Guidry, *"Modern General Relativity: Black Holes, Gravitational Waves, and Cosmology"*, first edition, Cambridge University Press, Cambridge (2019). 2

[2] N. Jarosik et al., *"The Astrophysical Journal"*, Supplement Series 192, 14 (2011), arXiv:1001.4744 [astro-ph.CO]. 2, 7, 50

[3] Planck Collaboration, P. A. R. Ade et al., *"Planck 2013 results. I. Overview of products and scientific results"*, Astronomy & Astrophysics 571, A1 (2014), arXiv:1303.5062 [astro-ph.CO]. 2, 7, 10

[4] B. Ryden, *"Introduction to Cosmology"*, Second Edition, Cambridge University Press, Cambridge (2017). 4, 7, 11, 24

[5] M. Lachieze-Rey; J.-P. Luminet, *"Cosmic Topology"*, Physics Reports, 254 (3): 135–214 (1995), arXiv:gr-qc/9605010. 5

[6] F. Melia, *"The apparent (gravitational) horizon in cosmology"* American Journal of Physics 86, 585 (2018); https://doi.org/10.1119/1.5045333. 5

[7] J. Higbie, *"Radial photon paths in a cosmic model: A student exercise"* American Journal of Physics 51, 1102–1107 (1983) https://doi.org/10.1119/1.13344. 6

[8] S. Jose, A. Leblanc, V. Faraoni, *"When can we compute analytically lookback time, age of the universe, and luminosity distance?"* The European Physical Journal C volume 82, Article number: 557 (2022) https://link.springer.com/article/10.1140/epjc/s10052-022-10519-2. 6

[9] A. Maeder, *"An Alternative to the ΛCDM Model: The Case of Scale Invariance"*. The Astrophysical Journal. 834 (2): 194 (2017). arXiv:1701.03964. 7

[10] A. Einstein, W. de Sitter, *"On the relation between the expansion and the mean density of the universe"*. Proceedings of the National Academy of Sciences. 18 (3) (1932). 7

[11] V. Rosenthal, *"From the Big Bang to the Big Crunch and Everything in Between A Simplified Look at a Not-So-Simple Universe."* iUniverse. p. 194. (2011) https://en.wikipedia.org/wiki/Special:BookSources/9781462016990. 8

[12] V. Sahni, H. Feldman, A. Stebbins, *"Loitering Universe"* Astrophysical Journal v.385, p. 1 (1992). 8

[13] R. Brandenberger, P. Peter, *"Bouncing Cosmologies: Progress and Problems"*. Foundations of Physics. 47 (6): 797–850. (2017) arXiv:1603.05834. 9

[14] A. R. Liddle, *"An Introduction to Modern Cosmology"*, John Wiley & Sons Ltd, Chichester (2003). 9

[15] R. A. Sunyaev, *"The thermal history of the universe and the spectrum of relic radiation"*. In Longair, M. S. (ed.). Confrontation of Cosmological Theories with Observational Data. IAUS. Vol. 63 (1974). 10

[16] D. Brout et al., *"The Pantheon+ Analysis: Cosmological Constraints"*. The Astrophysical Journal. 938 (2), 110 (2022). arXiv:2202.04077. 10

[17] S. E. Rugh, H. Zinkernagel , *"Weyl's Principle, Cosmic Time and Quantum Fundamentalism"*, Part of the The Philosophy of Science in a European Perspective book series (PSEP,volume 2) (2011). 12

[18] P. L. Chebyshev, *"Sur l'integration des diff´erentielles irrationnelles", J. Mathematiques (series 1)* 18, 87–111 (1853) 13

[19] C. W. Misner, D. H. Sharp, *"Relativistic equations for adiabatic, spherically symmetric gravitational collapse"* Phys. Rev. 136, 571–576 (1964) 36